

The Shelf-Edge Frontal Structure in the Central East China Sea and Its Impact on Low-Frequency Acoustic Propagation

Steven R. Ramp, Ching-Sang Chiu, Frederick L. Bahr, Yiquan Qi, Peter H. Dahl, James Miller, James F. Lynch, *Senior Member, IEEE*, Renhe Zhang, and Jixun Zhou

Abstract—Two field programs, both parts of the Asian Seas International Acoustics Experiment (ASIAEX), were carried out in the central East China Sea (28° to 30°N, 126° 30' to 128°E) during April 2000 and June 2001. The goal of these programs was to study the interactions between the shelf edge environment and acoustic propagation at a wide range of frequencies and spatial scales. The low-frequency across-slope propagation was studied using a synthesis of data collected during both years including conductivity-temperature-depth (CTD) and mooring data from 2000, and XBT, thermistor chain, and wide-band source data from 2001. The water column variability during both years was dominated by the Kuroshio Current flowing from southwest to northeast over the continental slope. The barotropic tide was a mixed diurnal/semidiurnal tide with moderate amplitude compared to other parts of the Yellow and East China Sea. A large amplitude semidiurnal internal tide was also a prominent feature of the data during both years. Bursts of high-frequency internal waves were often observed, but these took the form of internal solitons only once, when a rapid off-shelf excursion of the Kuroshio coincided with the ebbing tide. Two case studies in the acoustic transmission loss (TL) over the continental shelf and slope were performed. First, anchor station data obtained during 2000 were used to study how a Kuroshio warm filament on the shelf induced variance in the transmission loss (TL) along the seafloor in the NW quadrant of the study region. The corresponding modeled single-frequency TL structure explained the significant fine-scale variability in time primarily by the changes in the multipath/multimode interference pattern. The interference was quite sensitive to small changes in the phase differences between individual paths/modes induced by the evolution of the warm filament. Second, the across-slope sound speed sections from 2001 were used to explain the observed phenomenon of abrupt signal attenuation as the transmission range lengthened seaward across the continental shelf and slope. This abrupt signal degradation was caused by the Kuroshio frontal gradients that produced an increasingly downward-refracting sound-speed field seaward from the shelf break. This abrupt signal dropout was explained using normal mode theory and was

predictable and source depth dependent. For a source located above the turning depth of the highest-order shelf-trapped mode, none of the propagating modes on the shelf were excited, causing total signal extinction on the shelf.

Index Terms—Environmental acoustics, internal waves, Kuroshio current, shelf circulation.

I. INTRODUCTION

TWO major field programs were conducted during 2000–2001 near the continental shelf break in the central East China Sea (ECS) under the auspices of the Office of Naval Research (ONR) Asian Seas International Acoustics Experiment (ASIAEX) program. The primary ECS boundary interaction study, conducted during May–June 2001, was a three-ship operation involving the U.S. research vessel MELVILLE, and the PRC vessels SHI YAN 2 and SHI YAN 3. The entire experiment is summarized in several other papers [1], and elements of it are described here as necessary. Leading up to the 2001 experiment was a pilot study, conducted from the R/V REVELLE during 8 April to 2 May 2000. In this paper, elements of both experiments are combined to provide a detailed description of the multi-scale physical oceanographic variability at the ECS shelf edge, followed by two illustrations of how the mesoscale physical features can influence low-frequency sound transmission. The internationally approved study area for both field programs was a box bounded by 28° to 30°N, 126° 30' to 128°E which included a flat section of the continental shelf in the NW corner (95–150 m deep), the shelf break running diagonally across the middle from SW to NE, and a portion of the slope and deep basin (>2000 m deep) in the SE quadrant (see Fig. 1).

About 75% of the pilot study cruise time was spent mapping the bottom and sub-bottom with water guns, chirp sonars, and sediment cores [2]. This required the ship to steam very slowly (4 knots) along closely-spaced transects over the shelf. Underway physical oceanographic data were collected concurrently, and also during the remaining four days: An anchor CTD station was conducted the evening of April 10; and two CTD/ADCP transects were run across the shelf break on 18 and 24 April (see Fig. 2). Advanced Doppler sonars unique to the REVELLE were also operated continuously [3]. Oceanographic moorings were deployed at two sites at the beginning of the cruise and recovered near the end (see Fig. 2). All the moored instrumentation at the shallower site (Site 1) was lost to intense fishing activity.

Manuscript received December 17, 2003; revised July 23, 2004.

S. R. Ramp, C.-S. Chiu, and F. Bahr are with the Department of Oceanography, Naval Postgraduate School, Monterey, CA 93943 USA.

Y. Qi is with the South China Sea Institute of Oceanology, Guanzhou, PR China.

P. H. Dahl is with the Applied Physics Laboratory, University of Washington, Seattle, WA 98195 USA.

J. Miller is with the Department of Ocean Engineering, University of Rhode Island, Narragansett, RI 02882 USA.

J. F. Lynch is with the Woods Hole Oceanographic Institution, Woods Hole, MA 02543 USA.

Renhe Zhang is with the Institute of Acoustics, Chinese Academy of Sciences, Beijing, China.

Jixun Zhou is with the Georgia Institute of Technology, Atlanta, GA 30332 USA.

Digital Object Identifier 10.1109/JOE.2004.840842

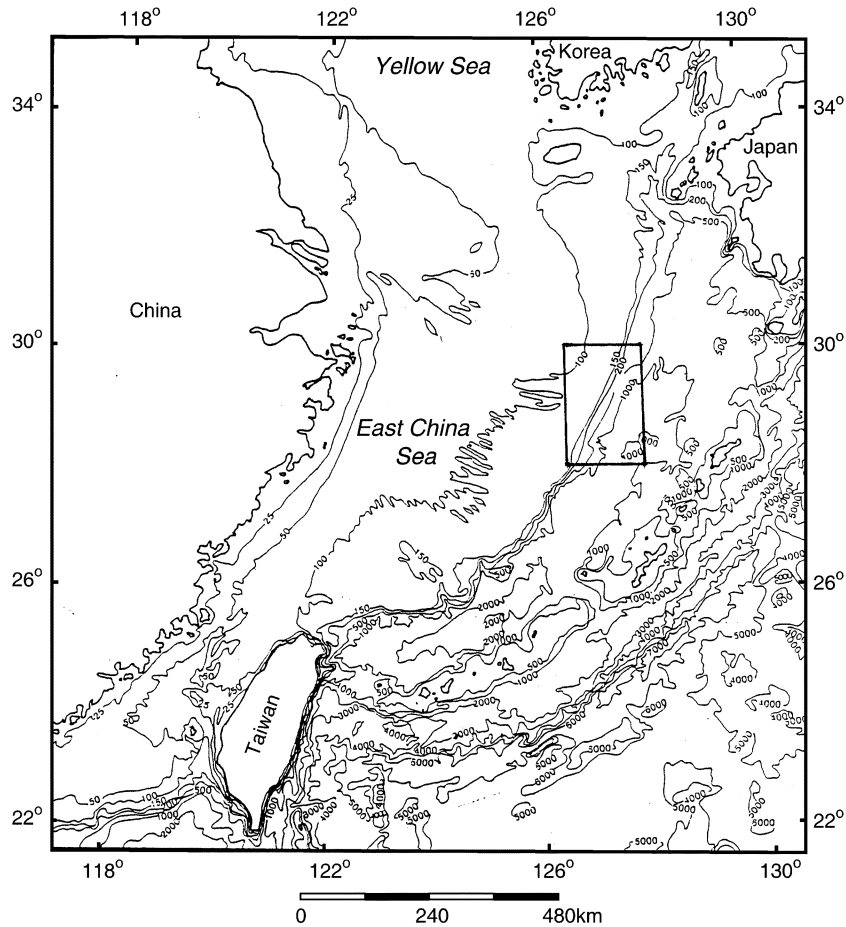


Fig. 1. Location of the ASIAEX East China Sea study region, showing the bottom bathymetry and relationships to the larger-scale surroundings.

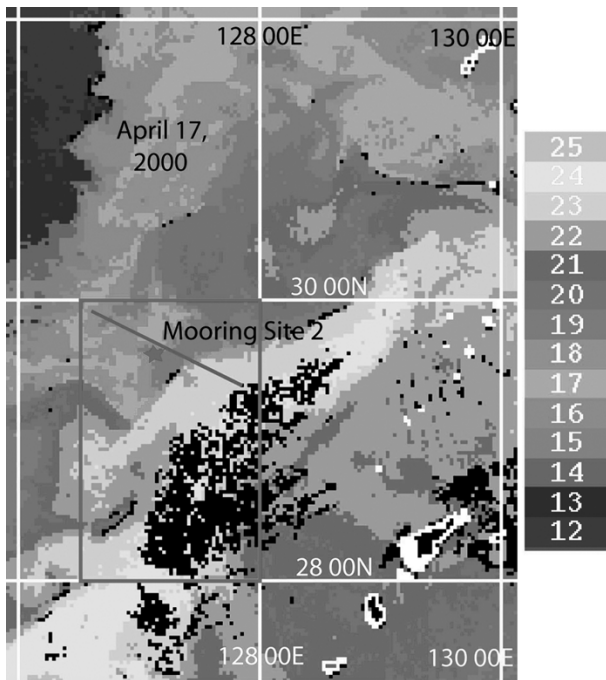


Fig. 2. The ASIAEX 2000 field configuration superimposed on a satellite SST image from 17 April 2000. Black pixels indicate contamination by clouds or low haze. The blue line indicates the across-shelf CTD transect referenced later. The color represents temperature in °C as indicated in the legend. The shelf water is indicated by the blue tones (12–13°C) and the Kuroshio surface water by the yellow and olive tones (21–24°C).

The primary 2001 data of interest to this paper were collected during the period of June 3–5, when operations from the MELVILLE were coordinated with those from the SHI YAN 2 and SHI YAN 3. Broadband acoustic propagation experiments were conducted over a twenty four hour period, during which the SHI YAN 2 deployed 38-g and 1-kg explosive sources at a depth of 50 m, at specified locations between 0.5 and 100 km from the MELVILLE and SHI YAN 3 (see Fig. 3). Data were recorded on various arrays deployed from the MELVILLE and SHI YAN 3, and operated by the Institute of Acoustics in Beijing, the Georgia Institute of Technology, the Harbin Engineering University, and the APL/UW and URI team. Sound speed measurements were made throughout the course of the experiment using CTD casts deployed from the MELVILLE, a thermistor chain and more CTD casts deployed from the SHI YAN 3, and XBT casts deployed from the SHI YAN 2.

The goals of this paper are as follows.

- 1) To summarize the physical oceanographic conditions at the ASIAEX ECS site as they pertained to the wide variety of acoustical studies conducted there during 2001 [1], [2], [4]. This includes principally the internal waves, tides, and Kuroshio variability.
- 2) To study specifically the impact of small filaments spun off from the Kuroshio on acoustic transmission loss on the continental shelf.
- 3) To understand the low-frequency acoustic propagation across the north wall of the Kuroshio Current in the East

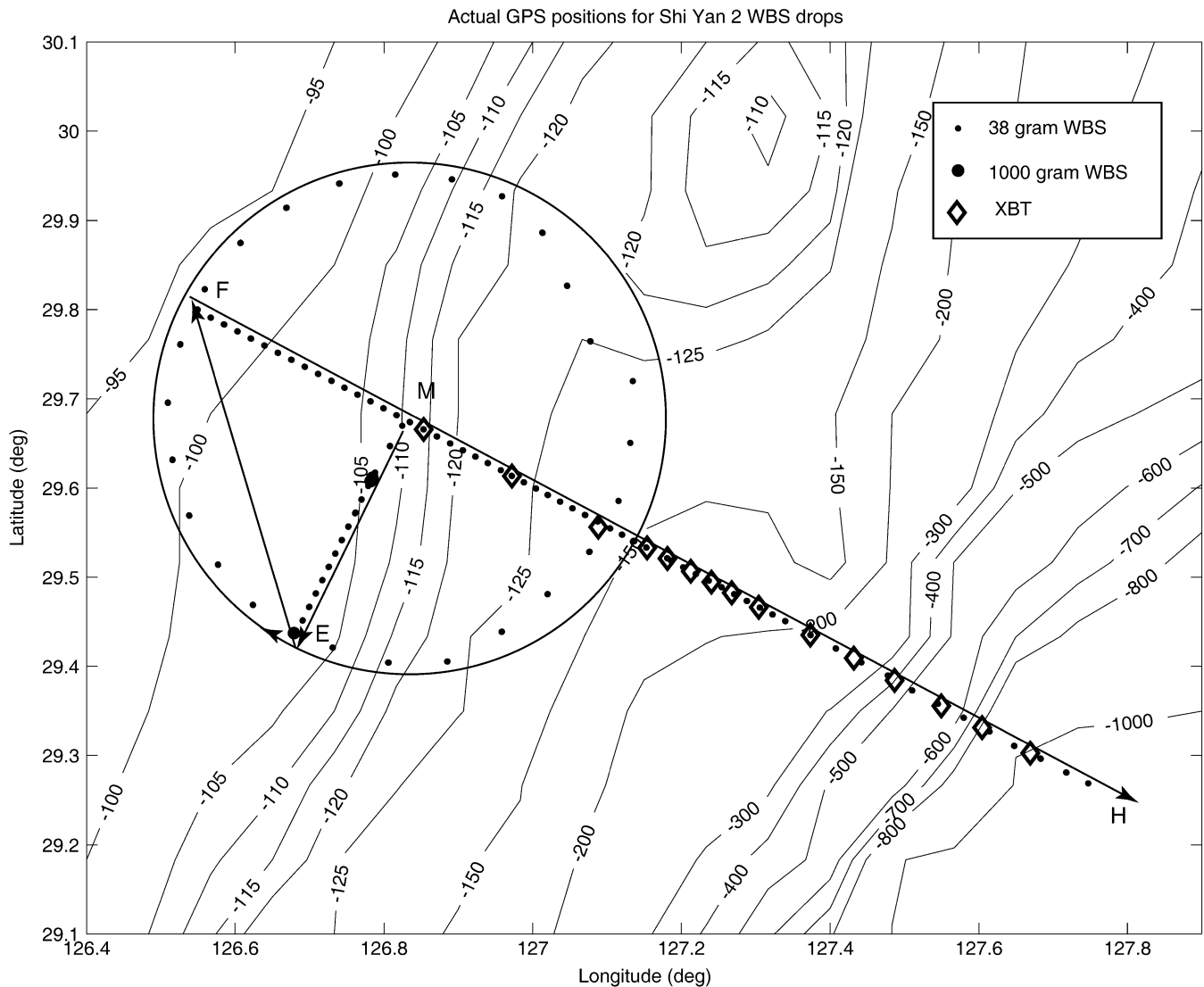


Fig. 3. Deployment patterns for the 38-g (small dots) and 1000-g (large dots) explosive charges used as broadband sources during the ASIAEX 2001 field program, as deployed by the Chinese ship SHI YAN 2. Fifteen Expendable Bathythermographs (XBTs) were also utilized along the line between waypoints M and H (diamonds). The listening arrays were deployed from the MELVILLE and SHI YAN 3 whose positions were near waypoint M at the center of the circle. The bathymetry data shown are from National Geophysical Data Center 5-Minute Gridded Elevation Data (ETOPO-5).

China Sea using a combination of observations and modeling.

The hydrographic and sound speed conditions during the 2000 REVELLE cruise will be described using an anchor-station CTD time series on the continental shelf and two CTD sections across the shelf and slope which spanned the strong temperature and salinity front on the north side of the Kuroshio Current. Some estimation of the variability of these parameters will be made using current and temperature data from a single oceanographic mooring at 125 m on the continental shelf. Then, under the assumption that there was little interannual variability in the deeper Kuroshio T/S relations, the 2000 CTD data over the slope and the 2001 Melville CTD data over the shelf are utilized in conjunction with a cross-shelf XBT section during 2001 to estimate the across-slope hydrographic (and sound speed) conditions during 2001. The acoustic model runs [5] will examine both the temporal variability on the shelf and

the Kuroshio frontal impacts, using the data sets described under 2) and 3) above.

This paper is organized as follows: Some background material on the physical oceanography of the ASIAEX ECS study region is presented in Section II. The data and methods for both 2000 and 2001 are presented in Section III. The oceanographic results from 2000 and 2001 are presented in Sections IV and V respectively, followed by the acoustic modeling in Section VI. The summary and conclusions section ends the paper.

II. BACKGROUND

The dominant oceanographic feature in the ASIAEX ECS box is the Kuroshio Current (hereafter KS). The KS enters the ECS between Taiwan and Yonakuni-jima, follows the continental slope very closely through most of the sea, separates from the slope near 30°N, and exits through the Tokara Strait. The entry point is quite complicated where the initially deep

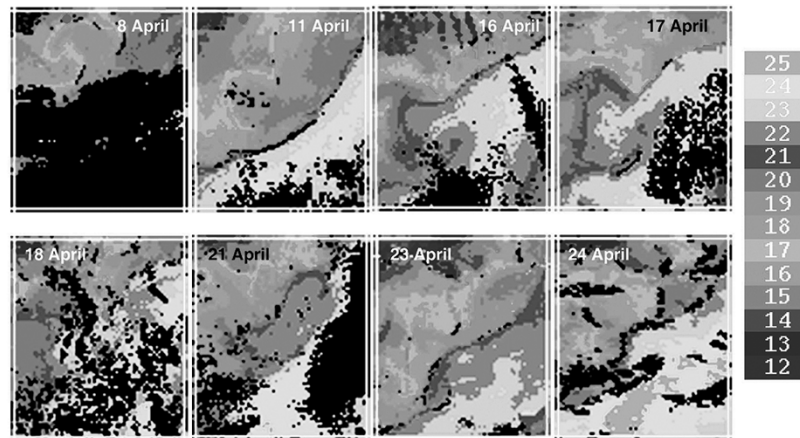


Fig. 4. Time series of eight satellite SST images of the ASIAEX region from 8–24 April 2000. All images have the same scale ($^{\circ}\text{C}$) as indicated by the color bar on the right-hand side. Black pixels indicate contamination by clouds or low haze. All frames are 2×2 degree lat/lon boxes bounded by $28\text{--}30^{\circ}\text{N}$, $126\text{--}128^{\circ}\text{E}$. The surface manifestation of the Kuroshio front is indicated approximately by the green-to-yellow (or brown) boundary. The anchor station conducted on April 9 is indicated by the red dot in the 8 and 11 April images.

KS collides with the continental shelf NE of Taiwan [6]–[9]. There is initially some overshoot, and a shallow “branch current” forms on the shelf with current speeds of only $15\text{--}20\text{ cm s}^{-1}$ [9] while most of the transport turns and follows the slope. Imagery suggests the branch current rejoins the main current a short distance downstream [6]. The flow along the slope in the central ECS is quite steady with little variation in the volume transport, which averages about $23 \pm 2\text{ Sv}$ in this region [10]. Ichikawa and Beardsley [10] found using 39 occupations of 6 across-shelf sections in the ECS that 75% of the transport is barotropic, and thus difficult to discern without direct current observations. The point where the KS separates from the continental slope is fairly constant, but may show some variation with volume transport, separating sooner during periods of high volume transport. This occurs during summer, when the transport may sometimes reach 40 Sv . The salient point with respect to this paper is that the current is always over the continental slope in the ASIAEX box, making this a good place to study the across-frontal acoustic propagation. With respect to the analogous Gulf Stream (GS) off South Carolina, the continental shelf is deeper and the edge of the KS much farther up over the shelf than in the GS case (James *et al.*, 1999). This makes it easier to span the KS front with acoustic sources than the GS. After separation, the current retroflects and exits the ECS via the Tokara Strait, where the volume transport increases dramatically due to the contribution from outside the Ryukyu Islands. The exit path of the KS is bimodal, with most of the current passing through either the northern or southern Tokara Strait, varying with a time scale of about 100 days [11].

Historical across-shelf sections of the temperature, velocity, and potential vorticity structure in the ECS show several features of interest to ASIAEX. From a section actually in the ASIAEX box, very close to the across-shelf acoustic propagation path, a double-thermocline structure has been observed, centered on 20°C and 15°C with a thermostad in between in the $17\text{--}18^{\circ}\text{C}$ range [12]. The lower thermocline extends up onto the continental shelf and seems to be upwelled from deeper within the KS itself, forming a warm, salty layer along the bottom. This upwelling and upslope transport of Kuroshio water also appears

in the tracer distributions from numerical models [13] and is presumably due to boundary layer effects beneath the KS. Several authors [14], [15] have observed a counter-current over the continental slope in this region, centered near 300 m with current speeds of $15\text{--}20\text{ cm s}^{-1}$ toward the southwest. This contrasts with maximum current speeds of about 110 cm s^{-1} toward the NE in the KS itself. Like most of the Gulf Stream, the mean potential vorticity gradients change sign across the KS, indicating the potential for baroclinic instability [14].

The above description of the steady state does not reflect the fact that the Kuroshio is an active western boundary current with propagating meanders, detached eddies, and warm filaments as it flows through the East China Sea. Using satellite and in-situ data, Qiu *et al.* [6] found $100\text{--}150\text{ km}$ wavelengths, $14\text{--}20$ day periods, and downstream propagation speeds ranging from $20\text{--}26\text{ cm s}^{-1}$ for the KS meanders along the shelf break in the East China Sea. A dynamical study of the KS meanders using both observations and a numerical model [15] quantified many characteristics of the KS meanders. Using an array of seven moored inverted echo sounders (IES), they found spectral peaks at 7, 11, and 16 days with the 11-day peak being the most persistent. The 11-day peak was also the most unstable (fastest growth rate) in the numerical model. The wavelength range was $195\text{--}265\text{ km}$, about like the Gulf Stream, but the GS has a dominant period of only 5.4 days and the meanders travel downstream much faster (order 40 cm s^{-1} vs. 20 cm s^{-1}) than in the Kuroshio. James *et al.* [15] attribute this to: 1) Position of the KS relative to the shelf break (10 km farther onshore); 2) Deeper continental shelf (165 vs. 50 m) in the ECS vs. the southeast U.S. continental shelf; and 3) Advection by the GS itself, which has a much higher transport (33 versus 20 Sv) off the southeast U.S. than the Kuroshio in the ECS. Basically, the Gulf Stream is more unstable due to greater shear across the front.

There are many other strong fronts in the Yellow and East China Sea [16] but none of them are likely to be observed in the ASIAEX box. The frontal positions in the region were compiled from satellite data using automatic processing algorithms [16]. Most of the ECS fronts are due to tidal mixing [17], including the Yangtze Bank front extending toward the SE over

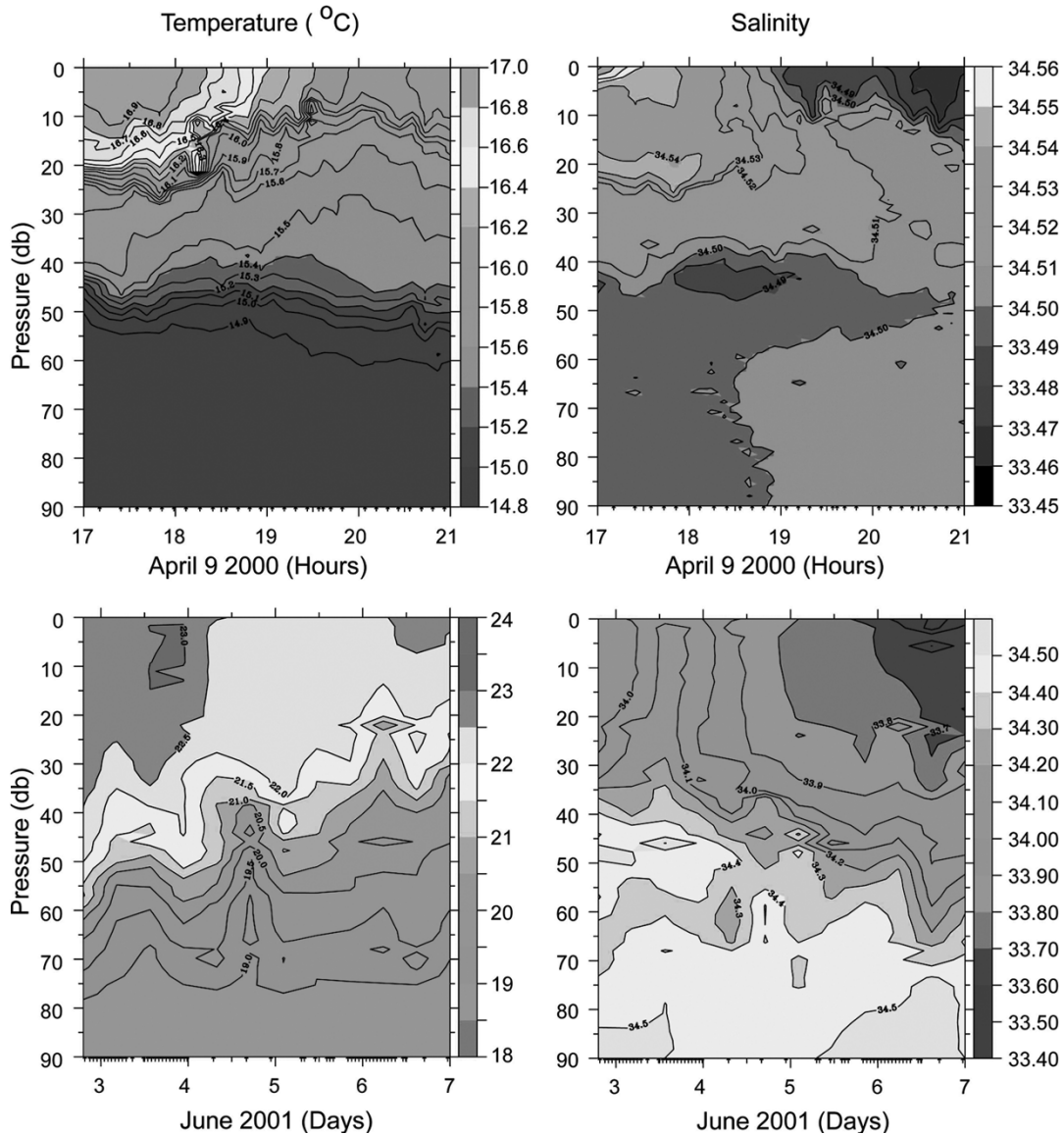


Fig. 5. Anchor CTD station of temperature and salinity from April 2000 (top) and June 2001 (bottom). Note the differing time scales on the two plots.

the shallow (less than 50 m) bank. There is an ample supply of Yangtze River outflow water over the bank [18] which creates this front when mixed to the surface by the tides. However, this front remains north of 30°N and does not likely impact the ASIAEX box. Thus, the fronts associated with the edge of the Kuroshio and its associated eddies and filaments are likely the only fronts which will impact the acoustic propagation in the ASIAEX study region.

The tides in the northern Yellow Sea are quite famous for their large amplitude and strong tidal currents [19] particularly in the Bohai Gulf, Seohan Bay, and Kyonggi Bay. The amplitude of these currents falls off rapidly however as the shelf break in the ECS is approached. Within the ASIAEX study region, the diurnal tidal constituents are small, less than 10 cm s^{-1} combined. The barotropic tides are mostly semidiurnal, with (u, v) amplitudes of $(26.7, 16.8)\text{ cm s}^{-1}$ for M2 and $(12.4, 7.8)\text{ cm s}^{-1}$ for S2. The semi-major tidal ellipse axes are oriented NW/SE across the topography suggesting ample opportunity for internal tide generation. In-situ observations of the internal waves and tides

however are sparse in the Yellow and East China Seas. Matsuno *et al.* [12] found wavelengths of 400 m for internal waves with periods less than 10 min. They found that the generation process was intermittent, and seemed to coincide with onshore shifts of the KS axis, which elevated the velocity shear over the shelf break and reduced the Richardson number below its critical level. Synthetic aperture radar (SAR) observations however [20] clearly show an abundant field of highly nonlinear internal waves (solitons) in the Yellow and East China Sea. At least one such wave was observed during the ASIAEX 2000 field program and is described in detail below.

III. DATA AND METHODS

A. April 2000

Many data sets were collected during the REVELLE spring 2000 ECS cruise but only those relevant to this paper are described here. The CTD data were obtained using an Sea-Bird

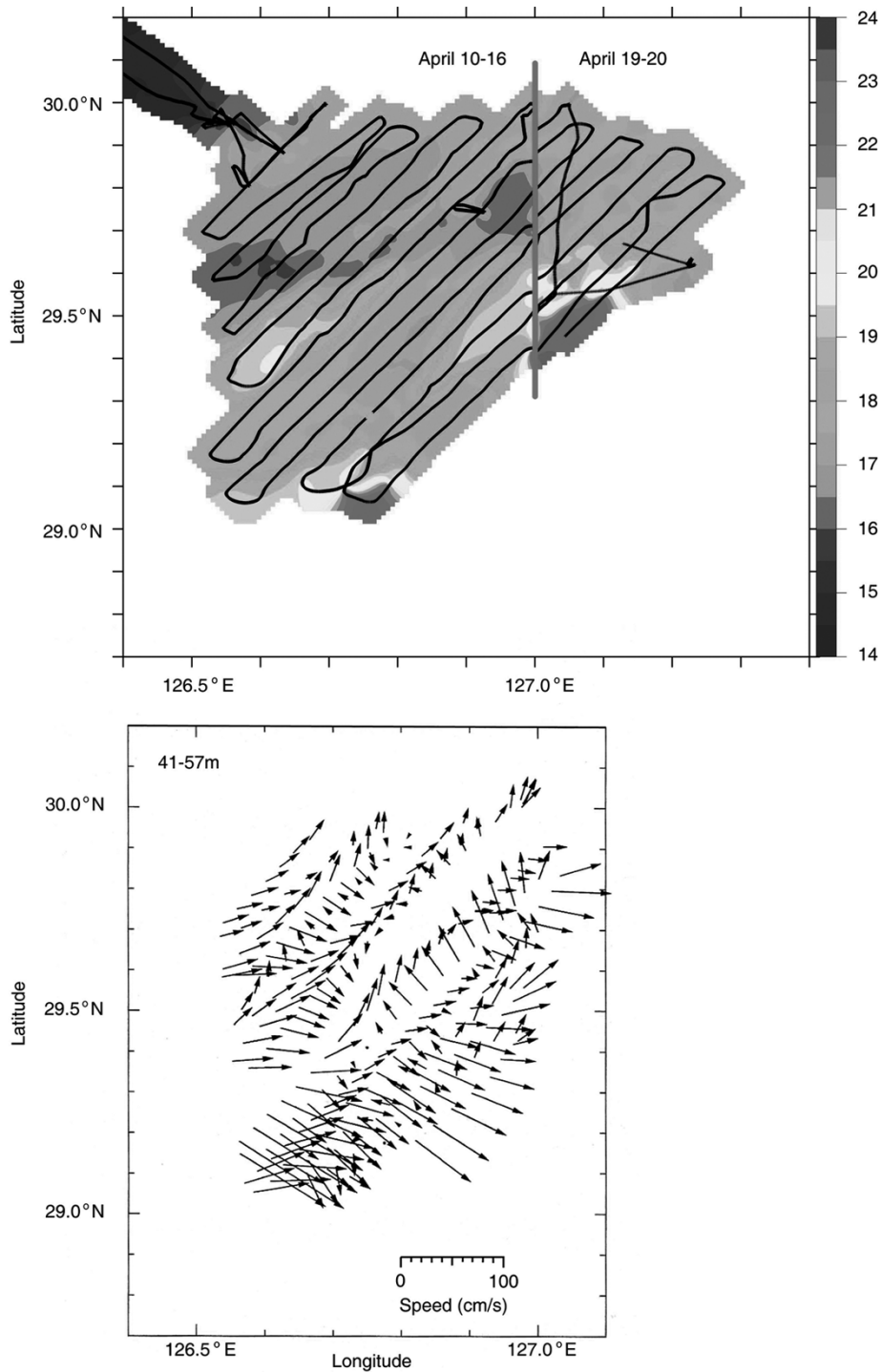


Fig. 6. Underway sea surface temperature ($^{\circ}\text{C}$, top) and ADCP velocity averaged over 41–57 m (bottom) as obtained from the R/V REVELLE during 10–20 April 2000. The vertical red bar represents a temporal discontinuity in the data collection, while the ship did other things.

Electronics, Inc., SBE 911+ CTD which was provided, maintained, and calibrated by the Scripps Institution of Oceanography. The instrument sampled at 24 Hz and was lowered at 30 m min^{-1} in shallow ($<100\text{ m}$) water and through strong vertical gradients and 60 m min^{-1} otherwise. The data were run through now standard processing algorithms to align the response times for the temperature and conductivity sensors and averaged to 1 dBar bins for presentation. Bottle salinity samples were collected at each station and run onboard using a

Guildline salinometer to maintain calibration. The CTD sampling was conducted as follows: 1) an anchor station consisting of 30 consecutive stations requiring roughly 20 minutes each located at $29^{\circ} 58' \text{N}$, $126^{\circ} 32' \text{E}$; 2) at each gravity core location; and 3) two occupations of a transect extending across the continental shelf from $29^{\circ} 55' \text{N}$, $126^{\circ} 37' \text{E}$ to $29^{\circ} 18' \text{N}$, $127^{\circ} 54' \text{E}$ (Fig. 2). During the first occupation on 18 April, 15 stations 9.2 km (5 nautical miles) apart were occupied along the transect. The second time during April 24, the station spacing was the

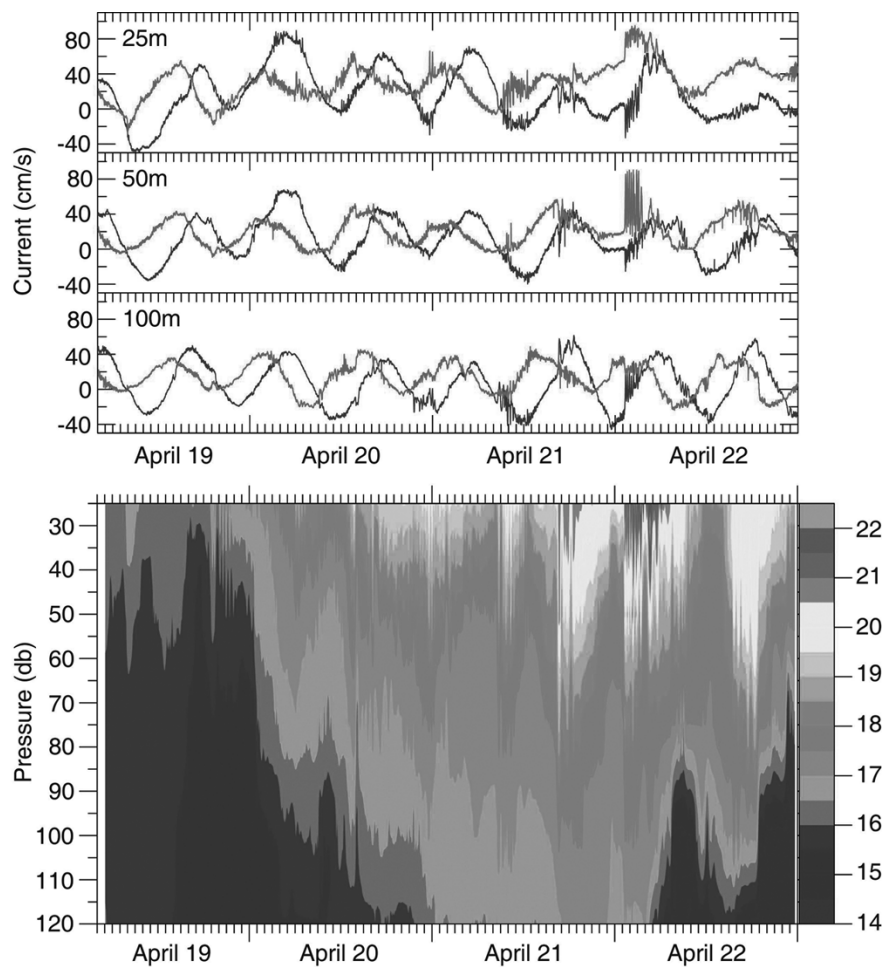


Fig. 7. (a) Time series of alongshore (red line, positive 30° east of true north) and across-shore (blue line, positive toward 120° east of true north) velocity from three current meters at 22, 50, and 100 m depth on the continental shelf in the East China Sea. The mooring location is as indicated by the red “X” in Fig. 2. The data are unfiltered and contain all frequencies of motion. (b) Contour plot of temperature ($^\circ\text{C}$) data from the same mooring as the velocity components shown in Fig. 9(a). The data were contoured from temperature time series collected at 25, 37, 52, 75, 100, and 120 m depth.

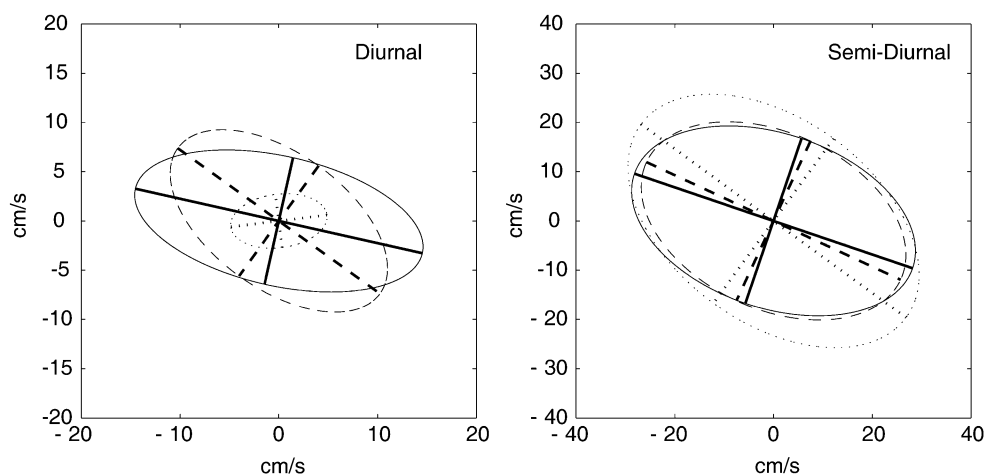


Fig. 8. Tidal ellipses for the diurnal (left) and semidiurnal (right) tidal bands from 22 m (solid line), 50 m (dashed line), and 100 m (dotted line) depth. The ellipses were calculated using harmonic analysis and the time series depicted in Fig. 7.

same but the three shallowest stations and the deepest offshore station were not occupied due to time considerations.

A hull-mounted RD Instruments, Inc., 150 kHz narrow-band acoustic Doppler current profiler (ADCP) was operated continuously throughout the cruise to collect vertical profiles of

horizontal ocean currents. The basic data set consisted of 5-minute averaged profiles sampled in 8-m bins from 17 m to nominally 350 m depth depending on sea conditions. The navigational input was from a Trimble GPS unit and an Ashtech DGPS unit to fine-tune ship’s heading, pitch, and roll. The

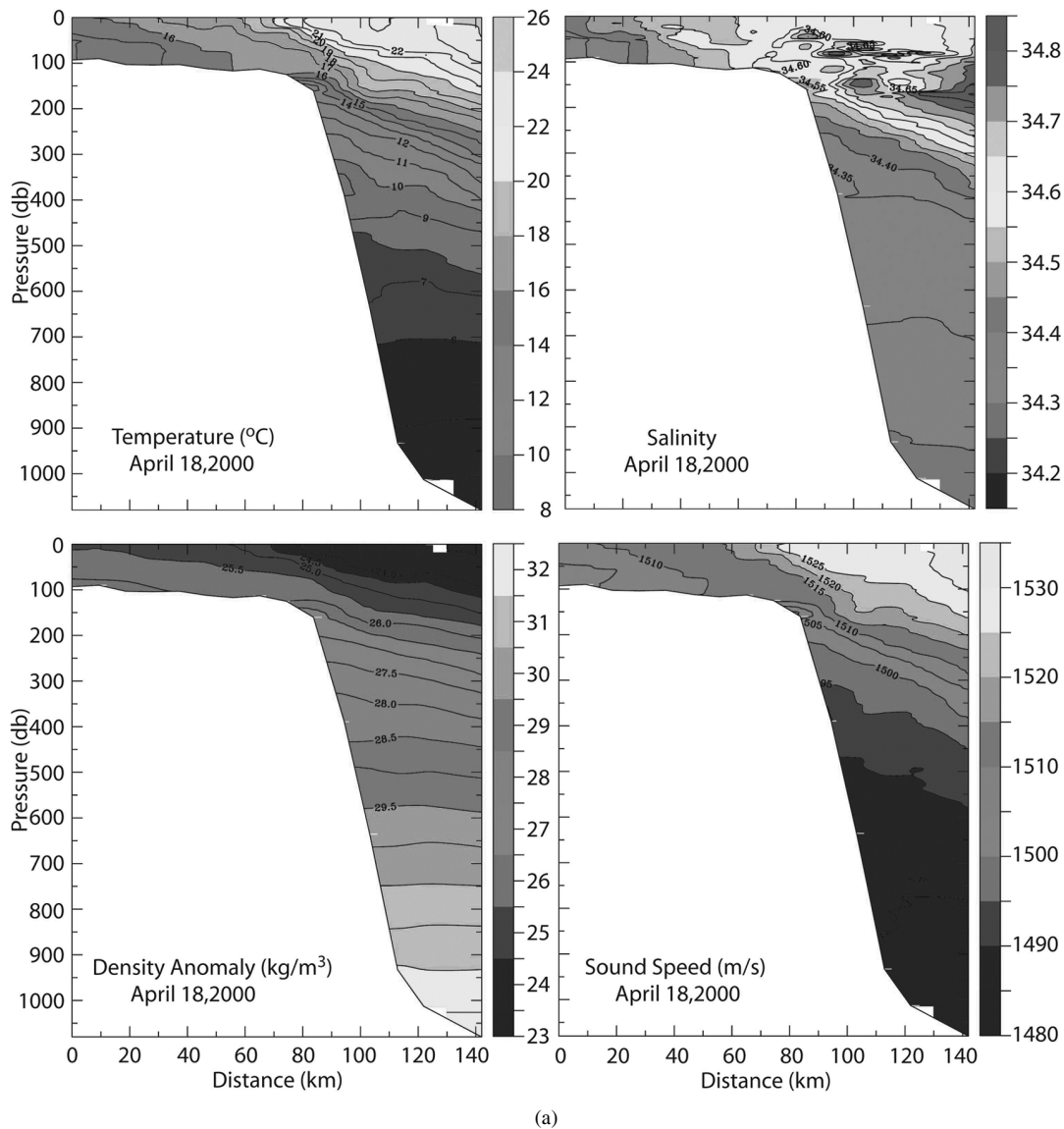


Fig. 9. (a) Temperature (top left), salinity (top right), density anomaly (bottom left), and sound speed (bottom right) along a section across the continental shelf in the ASIAEX region of the East China Sea on April 18, 2000. The data were collected along the section shown by the red line in Fig. 2.

data were processed onboard using the University of Hawaii's CODAS ADCP processing software which allows for rigorous quality control, navigation, compensation for transducer head offset, choice of reference layer, computation of absolute velocities, and data display.

Two sites were outfitted with moored instrumentation during ASIAEX 2000: The first, located near $29^{\circ} 55'N$, $126^{\circ} 37'E$ in 90 m of water, was completely lost to fishing activity. The second, deployed at $29^{\circ} 37.2'N$, $127^{\circ} 13.5'E$ on the 125 m isobath returned four days of good data from 19–23 April. The subsurface taut-wire mooring had three Aanderaa RCM-8 ducted paddle-wheel current meters sampling at 1-min intervals at 22, 50, and 100 m depth. Four Sea-Bird Electronics Inc. SBE-37 MicroCAT instruments also sampled at 1-min intervals at 25, 52, 75, and 120 m depth. A single mini-Starmon T-pod was moored at 37 m to fill in between the 25 m and 52 m MicroCATs. The instruments were all set to the maximum sampling rate to observe the internal wave field which could induce acoustical fluctuations. The location near the continental shelf break (see Fig. 2) and

just inshore of the Kuroshio front was ideal for this purpose. The current data were rotated 30 degrees clockwise, in line with the local shelf break bathymetry, to translate the east and north velocity components into an along- and across-shore basis.

The East China Sea satellite sea surface temperature (SST) data from the NOAA polar orbiting satellites were locally downloaded at 1-km resolution by the National Consortium for Ocean Research (NCOR) of Taiwan, ROC. The data were calibrated and navigated at NCOR and made available to the general public via their web site. Visibility was excellent during April 2000 and nine clear images were obtained to locate the Kuroshio front and other large-scale features during the experiment. Visibility during 2001 was quite poor and only a few small glimpses of the ocean were obtained.

B. June 2001

The three research vessels on scene collected myriad data sets during 2001 but with greater emphasis on the short-range (boundary interaction) problem than the across-slope (volume

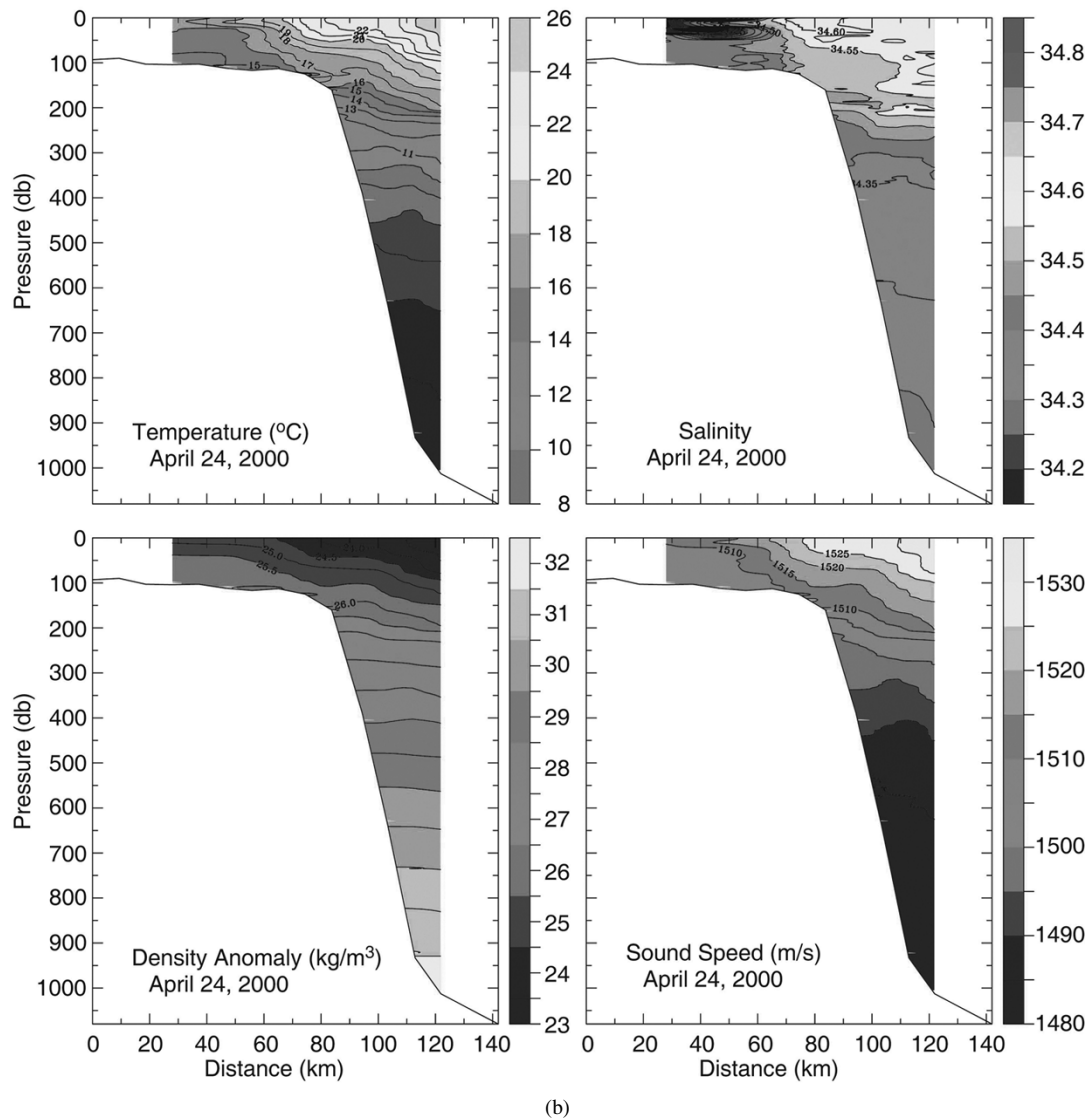


Fig. 9. (Continued.) (b) As in Fig. 9(a) but for April 24, 2000.

interaction) problem. The data collected are discussed thoroughly in data reports from the MELVILLE [21] and the two Chinese ships [22]. The data used in this paper are briefly summarized here for convenience.

Both the MELVILLE and the SHI YAN 3 were equipped with high-precision conductivity-temperature-depth (CTD) instrumentation. The SHI YAN 3 collected 54 CTD's at $29^{\circ} 40.47'N$, $126^{\circ} 49.21'E$ using an EG&G Mark IIIB CTD (see Fig. 3). This instrument sampled at 32 Hz and was lowered at about 1 m s^{-1} . The instrument was calibrated at the National Tianjin Gauge Station, PRC on 7 June 2001, immediately prior to the ASIAEX cruise. The MELVILLE CTDs were collected mostly using a Sea-Bird Electronics Inc. SBE 911+ CTD similar to the instrument used on REVELLE the year before. This instrument was also owned and calibrated by the Scripps Institution of Oceanography. Occasionally, when wire use conflicts developed, the CTD casts were made using a SBE 19+ SEACAT CTD owned and maintained by the Marine Physical Laboratory (MPL) of the Scripps Institution of Oceanography. The MELVILLE CTDs were mostly collected

as the ship held station at a single location near $29^{\circ} 39'N$, $126^{\circ} 49'E$, however a limited cross-shelf section of seven stations was made between $29^{\circ} 48'N$, $126^{\circ} 32'E$ and $29^{\circ} 36'N$, $127^{\circ} 01'E$ (see Fig. 3).

A 17-element thermistor chain suspended from the SHI YAN 3 also proved useful for characterizing the internal wave field. The T-chain had sensors spaced roughly every three meters apart from 20 to 80 m depth in 104 m of water. The data were collected for roughly 63 h between 0840 on 3 June to 0000 on 6 June.

While the MELVILLE and SHI YAN 3 held station with listening arrays deployed, the SHI YAN 2 steamed a circular pattern with 30 km radius around the two ships and made a cross-shelf transect offshore (see Fig. 3). The SHI YAN 2 was engaged in two principal activities during this time, namely deploying the 38 g and 1000 g explosive sources (called wide-band sources or WBS), and dropping expendable bathythermographs (XBT's). The WBS locations are shown by the dots in Fig. 3 and the type T-10 XBT's (good to 200 m depth) were dropped along the path between points M and H.

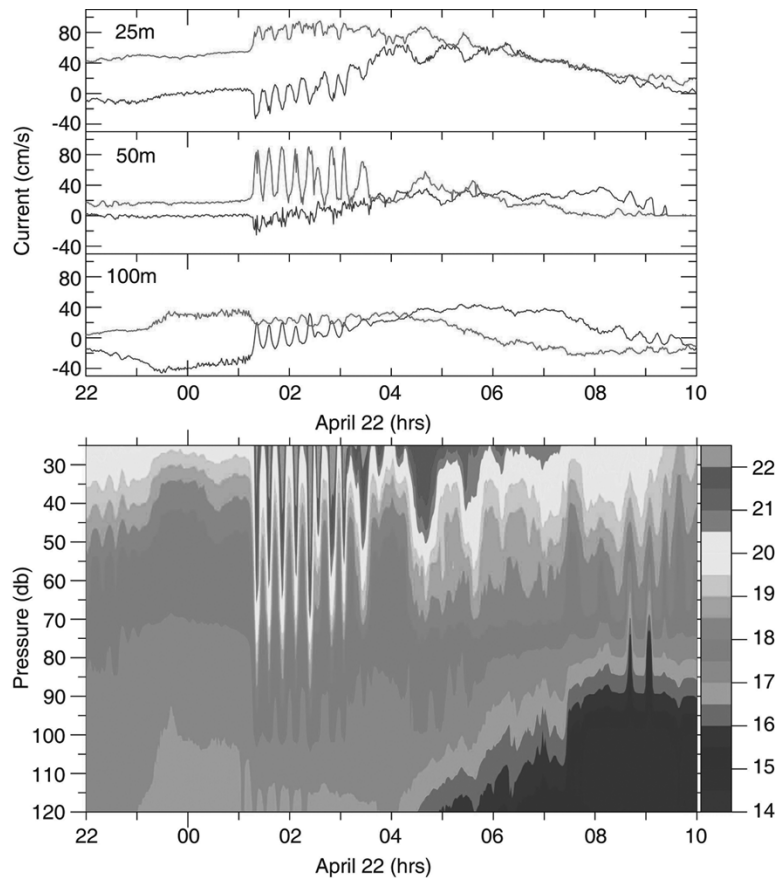


Fig. 10. As in Fig. 7 except the x-axis has been expanded to reveal the structure of the internal soliton event. The plots now show 12 h of data from 2200 on 21 April to 1000 on 22 April, 2002.

IV. APRIL 2000 RESULTS

A. Satellite SST

There were many clear SST images during April 2000 that helped frame the context of the experiment (see Fig. 4). From 8–11 April, a small eddy in the slope water advected out of the NW corner of the box. This was also apparent in the anchor station on 9 April (see Fig. 5) showing the temperature drop from 16.9°C to 16.0°C, accompanied by a salinity drop from 34.56 to 34.45 psu. The warm side of this small feature was only about 20 m deep (see Fig. 5). During 11–17 April, the Kuroshio front (as indicated by the green-to-yellow or brown boundary) moved onshore toward shallower water (northwestward) and looked ready to shed a small eddy or “shingle” (see Fig. 4). The feature never fully detached however, and on 18–21 April it re-coalesced with the main stream. The front then moved sharply southeastward on 21–23 April to a position aligned fairly close to the continental shelf break. There was little change in frontal position during 23–24 April. Additional evidence of all these frontal movements can be found in the *in situ* data that follow.

V. SPRING 2000 RESULTS

A. Shelf Conditions

The shelf conditions can be further characterized by the underway T/S and ADCP data, and by the four-day mooring at the 125 m isobath. The spatial variability at much higher resolution

than the satellite data are portrayed in the underway temperature and hull mounted ADCP data (see Fig. 6). The SST data ranged from <15°C in the NW corner to >22°C along the shelf break, where the Kuroshio overlapped the shallow topography. A warm (19°C) remnant of an earlier shingle was centered near 29° 20'N, 126° 55'E. The ADCP data show primarily semidiurnal tidal oscillations normal to the bathymetry with increasing amplitude toward the shelf break. There was some indication of meandering Kuroshio flow that correlated well with the warm (red) sections of the temperature plot. These flows reached 100 cm s⁻¹ along the southern boundary of the sampling region.

Despite their short length, the current meter records helped greatly in quantifying the shelf flow fields (see Fig. 7). The 4-day means were all alongshore, and slightly onshore, with speeds ranging from 34.4 cm s⁻¹ near the surface (22 m) to 14.0 cm s⁻¹ near the bottom (100 m). The primary variability was at the semidiurnal tidal period. With this short record, individual constituents could not be resolved, and the tides could only be divided generally into the diurnal and semidiurnal bands. The semidiurnal tidal ellipses at 22, 50, and 100 m depth had semi-major axis amplitudes of 30, 28, and 33 cm s⁻¹ oriented toward 161, 155, and 144 degrees, respectively (Fig. 8). The semidiurnal tide was therefore nearly uniform in amplitude and the ellipses rotated slightly counterclockwise with depth. The corresponding diurnal tidal ellipses at the same depths had amplitudes of 15, 13, and 5 cm s⁻¹ oriented toward 167, 144, and 7 degrees. This indicates a much more baroclinic tide than the semidiurnal band. At higher frequencies, there was a single burst

TABLE I
SUMMARY OF PROPERTIES OF THE ECS INTERNAL SOLITON PACKET

Amplitude (η_0)	40 m
Max Horizontal Current	70 cm s ⁻¹
Period (T)	15 min
Wavelength (λ)	500 – 800 m
Half Width (L)	~300 m
Number in Packet	8–9
Total Packet Length	~7 km

of internal wave activity during 0100 to 0330 on 22 April. The dynamics of this event span both the shelf and slope and will be described in greater detail in a separate section below.

The corresponding temperature records [see Fig. 7(b)] show that the mooring was deployed in the lightly stratified (16–17°C) shelf water as planned. During most of the record however the Kuroshio moved laterally onshore as indicated by the mean currents, increasing the temperature and stratification at all depths. Sometime late in the day on April 21, this motion reversed and the current began retreating offshore (see also Fig. 4). The internal tide is visible as a thermocline oscillation on top of the mean trends. The internal wave event of early 22 April was obvious in the temperature record as well as the velocity time series.

B. Slope Conditions

The two cross-shelf CTD sections on 18 and 24 April (see Fig. 9) illustrate the short-term variability across the north wall of the Kuroshio. The twin-thermocline structures [12] centered on 15 and 20°C and the thermostad in the 17–18°C range are clearly visible in both sections. The Kuroshio surface thermal front was manifested where the upper thermocline intersected the sea surface. The lower thermocline ran into the bottom near the shelf break. This resulted in a region of relatively low stratification right over the shelf break, which was more pronounced on the 18th than the 24th. The across-shelf positions of these fronts varied little between the two sections.

The salinity sections revealed the core of the Kuroshio and its cross-shelf position more clearly than the temperature sections. The Kuroshio core water ($S > 34.8$ psu) was centered near 150 m depth on 18 April. Several small parcels of high-salinity water were separating from the main stream over the continental slope, between 50–200 m depth. This water was absent on 24 April indicating a slightly more offshore position for the stream itself. This would agree with the satellite SST imagery (see Fig. 4) which showed the stream farther offshore on the 24th than on the 18th. The T and S changes over the shelf appeared to be compensatory as the isopycnals were nearly level there between 25.5 and 26.0 kg m⁻³. The total salinity variation in the sections was small, ranging only from 34.2 to 34.8 psu. As such, the sound speed in the upper ocean was mainly a function of temperature and the isotachs followed the isohalines closely in both cross-sections. The double-thermocline structure did not cause

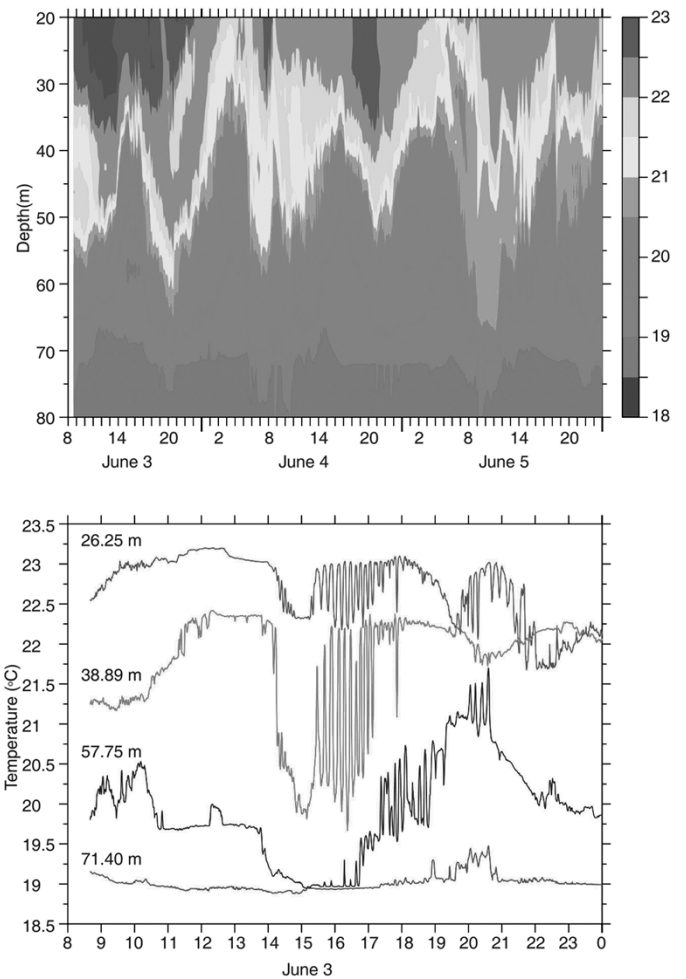


Fig. 11. Temperature contours from the T-chain deployed from the SHI YAN 3 while anchored at 29°40.47'N, 126°49.21'E. The dominant feature is a large-amplitude oscillation with a 12-hour period, attributable to the internal tide. Inset: An expanded-scale section of the plot for June 3, 2001. The color contours are from 26, 39, 58, and 71 m respectively. Note the internal wave packet from 1500–1700 h, with maximum amplitude at 39 m.

a double minimum in sound speed. Thus, while oceanographically interesting, this feature had little impact on the acoustic propagation.

C. Internal Waves

Of particular interest was a single burst of large, nonlinear internal waves observed on 22 April 2000. Recalling that in the rotated coordinate system, positive is offshore (southeast) and negative is onshore (northwest), these waves had onshore velocity in the upper layer and offshore in the lower layer [see Fig. 10(a)], indicating up-shelf propagation from the shelf break. The 50 m velocities were near the nodal point of a mode-1 internal wave and were primarily alongshore. The maximum velocity perturbations due to the waves approached 70 cm s⁻¹. The corresponding temperature records [see Fig. 10(b)] show these to be depression waves (forcing down the thermal structure) with a maximum temperature fluctuation of about +3°C between 37–52 m depth. The temperature and velocity structure of these waves identifies them clearly as a packet nonlinear internal solitary waves or solitons. There were 8–9

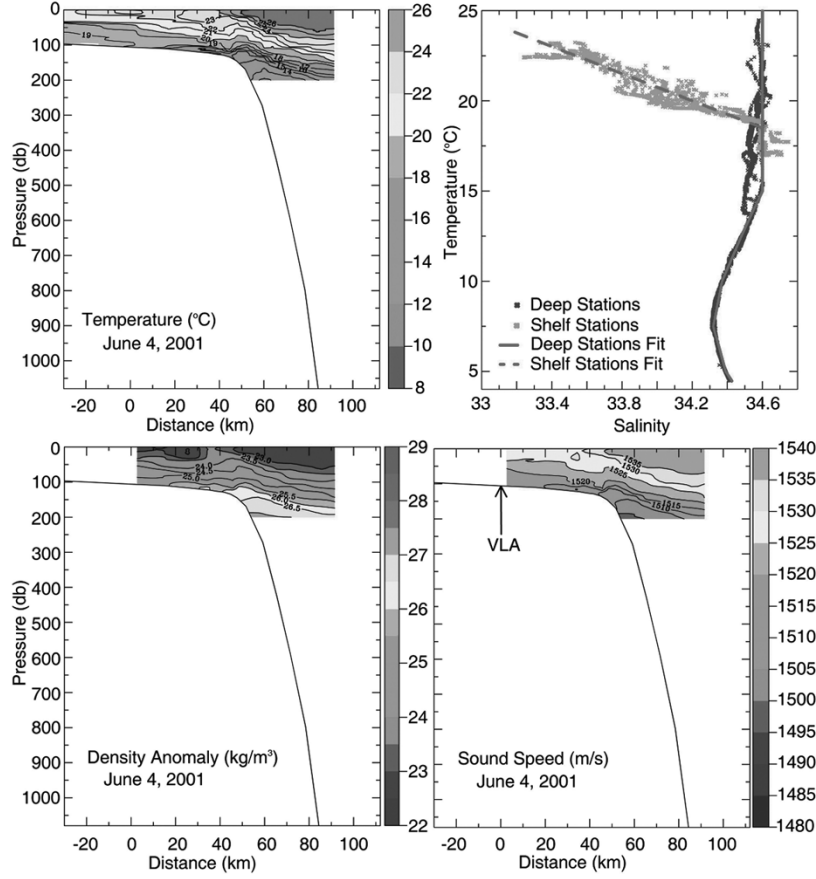


Fig. 12. (Top left) XBT section across the shelf and slope made by SHI YAN 2 during the WBS runs (see Fig. 3 for locations). (Top right) T/S relation used with the XBT data to compute the density section at lower left. (Bottom left) Density section computed using temperature from the XBT section and salinity from the T/S relation at upper right. (Bottom right) The synthesized sound speed section used to compute the model propagation loss across the shelf and slope during June 2001, computed from the density section at bottom left.

waves in the packet, spaced very regularly with a period of almost exactly 15 min. The wave amplitudes were calculated as

$$\eta'(t) = \frac{T'(t)}{\partial T / \partial z} \quad (1)$$

where T' are the temperature fluctuations at 37 m due to the wave and the vertical temperature gradient $\partial T / \partial z$ was computed as the difference between the smoothed temperature records at 25 and 52 m. Mooring motion was less than 1 m for this short mooring and was not a factor in the calculations. The first five waves in the packet had nearly equal amplitudes of about 40 m, with slightly less amplitude in the trailing three. Theoretically, soliton packets some distance from the source are rank ordered in space and time due to dispersion among the waves comprising the packet [23]. The fact that the first five waves were not rank ordered indicates that the mooring was very close to the generation region, i.e., the shelf break. With only one mooring and no SAR imagery available, the wavelength of the wave was not directly observed. It is possible, however, to make some estimate based on the REVELLE sonar imagery from the day before when a similar wave packet was observed and similar stratification prevailed (Luc Rainville, personal communication). The REVELLE crossed a group of four wave depressions in about 9, 9, and 6 min while transiting at 2.9 m s^{-1} , indicating separations of 1.6, 1.6, and 1.0 km, respectively. The ship however was transiting at an angle of 68° relative to the wave crests, which would actually indicate shorter

normal separations ranging from 500–800 m, not considering the propagation speed of the wave itself. Internal solitons also have the well-known property of creating alternating bands of smooth (slicks) and rough water on the sea surface above them [24]. These surface features were easily visible from the R/V REVELLE, and their spacing was consistent with the 500–800 m estimate above.

The soliton packet can also be approximated theoretically using simple 2-layer KdV theory [25], [26]. From Figs. 9(b) and 10, the upper and lower layer thickness h_1 and h_2 were 50 and 75 m respectively. The upper and lower layer densities ρ_1 and ρ_2 were 1024.5 and 1025.7 kg m^{-3} respectively, leading to a $\Delta\rho$ of 1.2 kg m^{-3} and reduced gravity $g' = 1.15 \times 10^{-2} \text{ m s}^{-2}$. The linear phase speed c_0 , quadratic nonlinear coefficient α , nonlinear phase speed c , dispersion coefficient γ , and half-amplitude width L for the solitons are then given by [26]:

$$c_0 = \sqrt{\frac{g'h_1}{1 + h_1/h_2}} \quad (2)$$

$$\alpha = \frac{3c_0}{2} \left(\frac{1}{h_2} - \frac{1}{h_1} \right) \quad (3)$$

$$c = c_0 + \frac{\eta_0 \alpha}{3} \quad (4)$$

$$\gamma = c_0 \frac{h_1 h_2}{6} \quad (5)$$

$$L^2 = \frac{12\gamma}{\eta_0 \alpha} \quad (6)$$

Substituting the values above and using $\eta_0 = 40$ m from the data yields a linear and nonlinear phase speed of 59 and 83 cm s⁻¹ respectively. The nonlinear phase speed in conjunction with the well-observed wave frequency of 1/900 s gives a wavelength estimate of about 750 m. This is not inconsistent with the estimate of 500–800 m based on the somewhat anecdotal observational evidence. The characteristic half-amplitude width from (6) = 137 m, compared to about 300 m from the data. The data estimate was computed using the displacement of the 20°C isotherm, with the time axis in Fig. 10(b) converted to space using an assumed constant phase speed 83 cm s⁻¹ e.g., [27]. Thus, the waves were somewhat wider than the 2-layer KdV theory would suggest. This suggests that higher-order (EKdV) nonlinearity may be a factor, as this tends to produce waves which are somewhat broader than the KdV theory in shallow water [26], [28].

The defining properties of the observed soliton packet are summarized in Table I. The waves were shorter (λ), smaller (η_0), higher frequency (f) and less dispersed than the Sulu Sea waves [23], [29] or the South China Sea waves [30], [31]. This is sensible as these other waves were generated at a remote sill and propagated large distances through deep water before being observed. The wave character is more in keeping with waves generated at the shelf break on the east coast of the United States [27], [32] as might be expected given the similar generation mechanism. The ECS waves had similar periods but much larger amplitude than the New England Shelfbreak PRIMER waves [27] possibly due to the stratification induced by the intruding edge of the Kuroshio Current.

How was this wave packet generated? Shelf-edge solitons are generally formed when the velocity of the off-shelf flow exceeds the free-wave speed and a hydraulic jump is formed [33]. On continental shelves in the ocean this generally occurs on the ebbing (off-shelf) tide. The jump thus formed is then released as an internal tidal bore when the tide turns, which quickly evolves into a packet of solitary waves. During the April 2000 ECS study, the free wave speed in the weakly stratified shelf water and near the bottom beneath the edge of the Kuroshio was about 42 cm s⁻¹. The total tidal current, i.e., the sum of the semidiurnal and diurnal ellipses (Fig. 8) was only about 38 cm s⁻¹, i.e., the off-shelf flow was sub-critical most of the time. During the early morning hours of 22 April, the Kuroshio shifted offshore, resulting in a total near-bottom off-shelf flow of about 50 cm s⁻¹ [see Fig. 7(bottom panel)]. The waves were released on the flood tide immediately following this event, which was apparently the only time during this short record when the off-shelf flow was strong enough to form a hydraulic jump and generate solitons. We conclude that both the tides and the Kuroshio meandering must both be favorable to generate solitons in this region of the East China Sea.

VI. JUNE 2001 RESULTS

The SHI YAN 3 was anchored at 29° 40.47'N, 126° 9.21'E during the experiment to allow maximum quieting for the acoustic observations. The CTD data sampled at this location during 3–7 June (Fig. 5(bottom)) show that the shelf water near the surface was significantly warmer and fresher than during April 2000. These changes can both be explained as seasonal effects:

The warmer temperatures in June (22–23°C) were likely due to solar insolation in late spring and summer. Salinities in the upper 25 m of the water column ranged from 33.6 to 34.0 psu as opposed to 34.45 to 34.56 psu the previous April (see Fig. 5). The bottom layer salinity was about the same during both years at 34.5 psu. The upper layer freshening was likely due to the seasonal southward spreading of the Yangtze River Plume which reaches its maximum in July [18], [34]. Thus fresher waters are expected over this region of the shelf during June than in April.

The T-chain data from the SHI YAN 3 provide some information on the temporal variability (see Fig. 11). The semidiurnal internal tide oscillating vertically on the strong, shallow thermocline was the dominant signal observed in this record, which looks much different than the 2000 data. This strong thermocline had not yet developed over the continental shelf during April 2000. The internal tide sometimes elevated 19°C water all the way to the surface as for instance during 0000–1200 on June 5, 2001. This created very strong horizontal fronts in the mixed layer at this time which would likely influence acoustic propagation. The internal tide therefore represents a significant source of uncertainty when using mean across-shelf sections to compute the spatial structure of the acoustic propagation.

Also of interest is the structure of the high frequency internal waves. There were two bursts of internal wave activity recorded, the strongest one between 1500–1700 hours on June 3, 2001 [see Fig. 11(bottom panel)]. These waves were oscillatory with a period of about 10 minutes. They did not resemble the strongly nonlinear internal solitons observed during April 2000. Thus, it appears quite special conditions must exist at the shelf break for the nonlinear waves to be generated. The linear internal waves observed during June 2001 caused fluctuations of 2°C in the thermocline (corresponding to an amplitude displacement of less than 10 m) as opposed to $T > 3^\circ\text{C}$ and amplitude >40 m during April 2000.

The XBT section (to 210 m depth) collected by the SHI YAN 2 during the WBS run across the continental shelf and slope did a good job of depicting the across-slope position of the Kuroshio front [see Fig. 12(top left)]. The surface front was located over about the 150 m isobath, similar to April 2000. The thermocline fluctuations were likely due to the internal tide as shown by the T-chain data. There appeared to be an upwelling feature over the shelf break below the inshore edge of the Kuroshio, similar but more pronounced than during spring 2000. There was a two-layer structure over the continental shelf, with a strong thermocline at about 38 m. The surface and bottom boundary layers were both about 20 m thick and well mixed. The bottom boundary layer was almost exactly 19°C at 34.5 psu and the surface layer between 22.0–22.5°C with varying salinities. The inshore end of the XBT section shows a thermal inversion with 18.5°C water above the 19.0°C water in the BBL. This feature was also observed at the inshore end of the MELVILLE CTD section near the same location (not shown). The water column was statically stable due to the strong salinity gradient with much fresher water over the 34.5 psu water. This thermal inversion may be a common feature during the summer months near the southern extremity of the Yangtze River Plume.

The lack of salinity data along the WBS transect was a problem, since the salinity variations may be important when

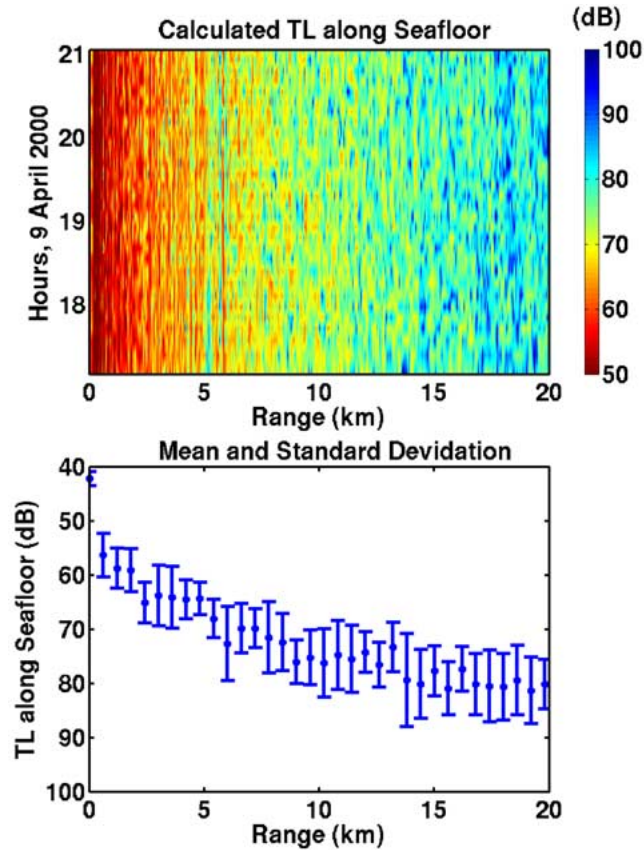


Fig. 13. Modeled warm filament-induced temporal fluctuations in the TL along the seafloor for a 1-kHz CW transmission, showing large standard deviations. Source depth in the synthesis is 20 m. The input sound speed fields were derived from the CTD time series shown in the top panels of Fig. 5, and the standard deviations were estimated from the modeled TL time series spanning a period of four hours.

determining the absolute sound speed across the shelf and slope, particularly up on the continental shelf. To determine the across-shelf sound speed structure, a T/S relation was needed to synthesize salinity profiles from the XBT temperature profiles. These synthetic “CTD casts” could then be used to compute the sound speed variability along the WBS transmission paths, a primary input necessary for the propagation loss modeling. Two data sets were used to compute this T/S relation: In the offshore Kuroshio water, there was a reasonably tight T/S curve available from the 2000 pilot study cruise on the REVELLE [see Fig. 12(top right)]. The assumption was made that this T/S relation had little inter-annual variation between 2000 and 2001 and these data were used to compute the salinity profiles in water deeper than 145 m. Over the shelf, the T/S relation from the 2001 data from the short MELVILLE across-shelf section was used (Fig. 12(top right)). The bottom layer water had a salinity near 34.5 psu, similar to the year before. The surface layer salinity decreased onshore from 33.5 near the 125 m isobath to less than 32.8 psu at the inshore end of the section.

This combined T/S relation was used to compute the density and across-shore sound speed structure during June 2001 [see Fig. 12(bottom)]. This sound speed section is the one actually used for the acoustic propagation loss modeling. Since the section was terminated at the receiving arrays located at the center of the circle, and the thermal inversion was only observed NE of there, the inversion does not appear in the final transect. The model-predicted propagation loss was calculated along the

transect and the results were compared with the observed propagation loss from the WBS drops as the SHI YAN 2 steamed offshore. These results are discussed in detail in the following section of the paper.

VII. ACOUSTIC MODELING

The purpose of this paper is to provide a detailed description of the multi-scale physical oceanographic variability in the ECS shelf edge and to illustrate the impact of the mesoscale variability on low-frequency sound transmission. The acoustic influences of the internal tides and waves are not discussed here. Readers who are interested in those finer-scale effects are referred to other papers on the subject in this issue.

Specifically, the acoustic studies presented in this paper were designed to investigate the following.

- The variance induced by the observed warm filaments shed by the Kuroshio Current in the transmission loss (TL) along the seafloor in the NW quadrant of the ECS ASIAEX box where the reverberation experiment took place. We believe that an understanding of this induced TL variance is important to the interpretation of the reverberation data, for example, in obtaining accurate estimates of the bottom scattering strengths.
- The observed phenomenon of abrupt signal loss as the transmission range lengthens seaward, passing the shelf break, in a cross-front transmission. This abrupt and

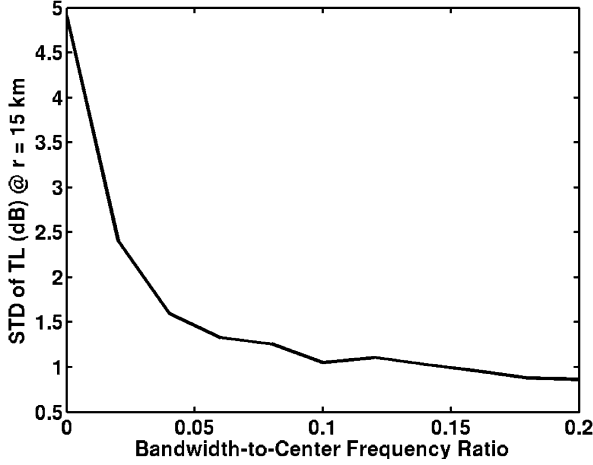


Fig. 14. Standard deviation of TL versus signal bandwidth computed from model simulations. The curve shown is for a range of 15 km on the seafloor.

severe signal degradation is caused by the Kuroshio frontal gradients that produce an increasingly downward-refracting sound-speed field seaward from the shelf break. We shall explain this abrupt signal dropout using normal-mode theory, and show that the range where this occurs is predictable and is source depth dependent.

A. TL Variance

Is acoustic propagation in the NW quadrant of the ASIAEX box robust to mesoscale volume variability? To answer this question, the CTD yoyo data collected in the pilot experiment were used to quantify the variances in the TL through acoustic modeling. Note that all the acoustic calculations discussed in this paper were performed using the coupled normal-mode model of Chiu *et al.* [5]. The CTD anchor station [see Fig. 5(top)] has captured the temporal variations of temperature and salinity in the water-column caused by the movement of a warm filament in the NW quadrant over a period of several hours. The observed temperature variations are mild, only about 1°C in the upper 30 m in 4 hrs. This temperature change corresponds to a change in sound speed of approximately 3 m s⁻¹ over the same period.

In synthesizing the TL fluctuations and their statistics, a source depth of 20 m and a center frequency of 1 kHz were used. The rationale behind picking a frequency of 1 kHz for the synthesis was that the primary sound source planned for the main bottom interaction experiment was small explosives that would emit a dominant portion (80%) of the signal energy in the low-frequency band below 1 kHz. Since the variance of TL generally increases as frequency increases, the 1-kHz results would correspond to a conservative, upper bound estimate. The 20-m source depth was also picked for the same reason to establish a worst case, since this depth is at approximately where the observed sound speed exhibits the most fluctuations. Additionally in the synthesis, we assumed that the water-column sound-speed field, derived from the CTD time series using an empirical formula, is a function of time and depth only, i.e., range-independent, over the distance considered. The modeled propagation path is 20 km in length and has a north-south orientation. The bottom depths used were extracted from echo-sounding data. The depths only change slightly from 94

to 100 m over the entire path. The sediment was assumed to be a homogenous layer with a sound speed of 1620 m s⁻¹, density of 1900 kg m⁻³ and attenuation rate of 0.1 dB m⁻¹ kHz⁻¹. These numbers correspond to average values deduced from the core measurements [2]. A more precise sediment model was not available at the time of this study. However, these simplified sediment parameters should be adequate for investigating TL fluctuations caused by volume variability.

Transmission loss is a relative measure of power loss for periodic signals, and of energy loss for pulsed (broadband or band-passed) signals, during their transmission from the source to the receiver. Given transmitted signal $s(t)$, i.e., sound pressure at 1 m from the source, and received signal $r(t)$, whose Fourier transforms are $S(f)$ and $R(f)$, respectively, the transmission loss is defined in general as

$$TL = -10 \log \frac{\int_T r^2(t) dt}{\int_T s^2(t) dt} \quad \text{or equivalently} \\ -10 \log \frac{\int_{-\infty}^{+\infty} |R(f)|^2 df}{\int_{-\infty}^{+\infty} |S(f)|^2 df} \quad (7)$$

where the integration time T is either the signal period for a periodic signal transmission, or the duration of the received signal for a pulsed transmission. For a modeled (i.e., known) sound channel transfer function H that is dependent on frequency f , source position \vec{x}_0 and receiver position \vec{x} , TL can be evaluated as

$$TL = -10 \log \frac{\int_{-\infty}^{+\infty} |S(f)|^2 |H(f, \vec{x}_0, \vec{x})|^2 df}{\int_{-\infty}^{+\infty} |S(f)|^2 df}. \quad (8)$$

Using the above equation, we shall first examine the TL variances along the seafloor in the modeled CW transmission. Examination of the TL variances associated with a bandpassed signal with increasing bandwidth shall then follow.

For a CW signal, $S(f)$ is a delta function and hence TL reduces simply to $-10 \log |H(f_o, \vec{x}_0, \vec{x})|^2$ where f_o is the carrier frequency. This modeled single-frequency TL structure is seen to consist of significant fine-scale variability in time caused primarily by the changes in the multipath/multimode interference pattern (see Fig. 13). The interference is quite sensitive to small changes in the phase differences between individual paths/modes induced by the evolution of the warm filament. The resultant standard deviations at various ranges are about 4–5 dB. Considering the mildness of the volume variability, this result is quite alarming and it warrants an exploration on possible variance reduction through an increased bandwidth.

For the case of a bandpassed (i.e., pulsed) signal with a flat source signal spectrum over its bandwidth Δf , (2) reduces to

$$TL = -10 \log \frac{\int_{f_o - \Delta f/2}^{f_o + \Delta f/2} |H(f, \vec{x}_0, \vec{x})|^2 df}{\Delta f}. \quad (9)$$

Thus, the processing of a bandpassed signal corresponds to a bandwidth-averaging (smoothing) action. Fig. 14 shows the changes in the standard deviation of the TL at the seafloor at a range of 15 km as the bandwidth is varied in the simulation. The standard deviation is seen to reduce exponentially as bandwidth

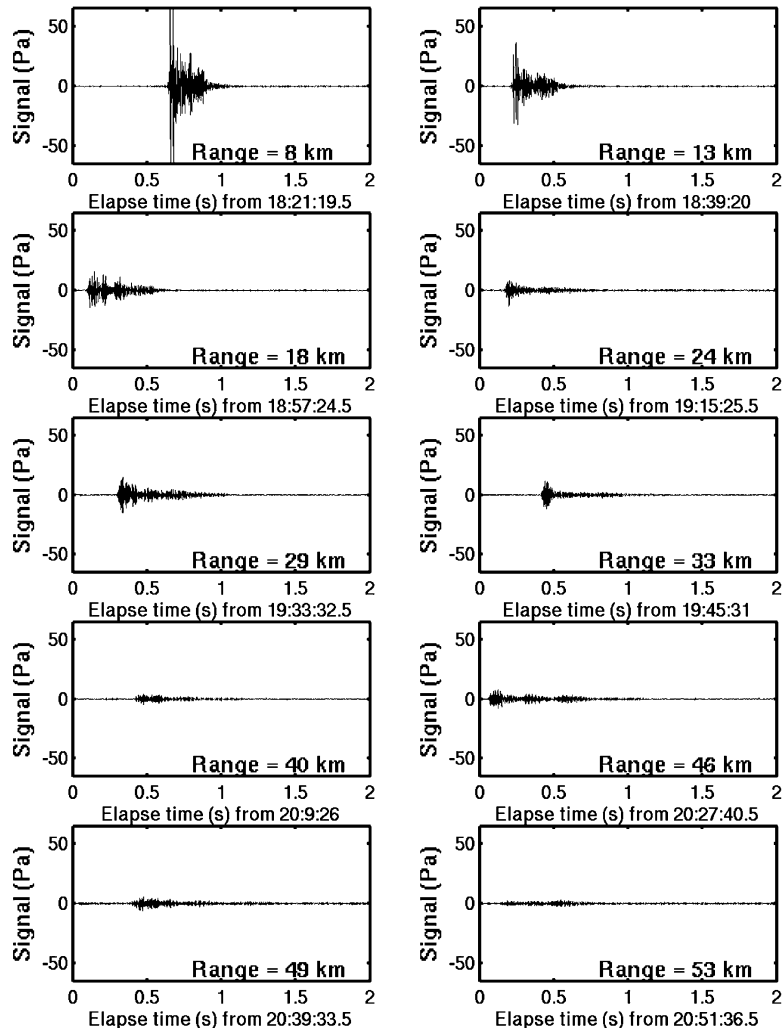


Fig. 15. Explosive signals recorded by the hydrophone at a depth of 83 m on the shelf for various source ranges during the cross-front propagation experiment in 2001. Data shown have been bandpass-filtered to improve SNR. The pass-band used is 100–300 Hz.

increases and it drops to less than 1 dB at a width of 200 Hz or 20% of the carrier frequency. All other ranges exhibit similar variance reductions in the TL. This is an interesting result in that it suggests: Even without adequate monitoring of the volume variability in the NW quadrant, accurate analysis of the boundary reverberation in this designated area is achievable through the use of bandpassed signals in large enough bands.

This numerical result is entirely consistent with the theoretical results of Dyer [35] and Makris [36]. Considering phase-random multipaths in saturated propagation, Dyer showed theoretically that TL (aside from a multiplicative constant) should exhibit fluctuation statistics that obey the exponential-gamma distribution [35]. Dyer then went on to show that for a single tone, this distribution has two degrees of freedom and a standard deviation of 5.6 dB, and that as the number of degrees of freedom (which is twice the number of independent tones L) increases, the distribution narrows as its standard deviation asymptotically approaches zero. Reformulating the theory but in terms of the number of coherence cells μ in the integration time (i.e., the intrinsic time-bandwidth-product), Makris arrived at the same distribution and the same dependence of the standard deviation if μ and L were

interchanged [36]. This is not surprising since both μ and L carry the same meaning, in a statistical sense, as the number of independent random variables/intensities. A comparison of the numerical results displayed (see Fig. 14) to the theoretical curve derived by either Dyer or Makris reveals that the number of independent intensities increases from one to about twenty as the bandwidth increases from zero to 200 Hz for the modeled shelf sound channel consisting of filament-induced fluctuations.

B. Abrupt Signal Loss

During the 2001 experiment, a set of 38-g explosive wideband sources were systematically deployed seaward across the continental shelf and slope from a vertical hydrophone array (VLA) stationed on the shelf (see Fig. 3). The array having 14 equally spaced hydrophones occupying the depths from 35 to 87 m was tethered from R/V MELVILLE near Waypoint M, and the explosive sources were cast from R/V SHI YAN 2 as she steamed toward Waypoint H. The depths of detonation were reported by Peng *et al.*[22] to be 50 m, who also provided a reliable estimate of the source level including its variability as a function of frequency based on seven independent detonations in close proximity to a calibrated receiver. The seven realizations show

small standard deviations of 0.5 dB or less in the octave band levels up to 1 kHz and higher, indicating that the signals produced by these explosives were highly repeatable.

The recorded VLA data were first calibrated to have sound pressure units using the known -156 dBV re $1 \mu\text{Pa}$ receiver sensitivity. The calibrated data showed that a significant amount of the signal energy was confined between 100 and 300 Hz, as anticipated given the source spectrum combined with attenuation of the higher frequencies. The signal in the 300 to 400 Hz band was also contaminated by tonal noise from the dynamic positioning system on the R/V MELVILLE [21]. Due to these circumstances, the identification and extraction of the explosive signals were facilitated by first band-passing the data using a Butterworth filter with low and high frequency cutoffs at 100 and 300 Hz. The filtered time series has a much-improved signal-to-noise ratio (SNR), disclosing that not all the explosive sources deployed were detonated. Additionally, vertical beam-forming was also performed to aid in the identification of weak signals for ranges beyond 50 km. However, no signal above the beam noise was detected beyond a range of 58 km from the vertical array, despite 20 additional WBS sources out to a range of 90 km being deployed. The identified, band-passed explosive signals recorded by one of the hydrophones of the VLA for various ranges (see Fig. 15) shows a decaying trend in the signal amplitude with range, and the signal from 54 km away and beyond was so weak that it was barely above the noise level. To permit a quantitative estimate of signal energy loss versus range, all the identified signals in the pass-band were squared and then time integrated. After accounting for the source level of 207 dB re $1 \mu\text{Pa}^2$ for the frequency band under consideration [22], and the spread of the signal duration, which expands to 1 s at 50 km and beyond from 60 ms at the source, the transmission loss (TL) estimates were determined (see Fig. 16). The observed TL clearly shows an abrupt and severe increase (or drop) in the energy level, between 54 and 58 km.

In an attempt to model this abrupt signal degradation, the sound-speed field developed from the XBT survey (see Fig. 12) along this acoustic track was employed along with the bathymetry that was analyzed from echo sounding measurements collected by the R/V SHI YAN 2 [22]. Below 200 m in the slope region where the XBT survey provided no coverage, CTD measurements from previous years were used to fill in the water-column sound speeds there. The notable feature in the figure is the inshore edge of the Kuroshio Current at a range of about 50 km from the VLA. In the absence of a more precise model for the geoacoustic parameters, the homogenous-layer, first-cut model was adopted once again for this modeling investigation.

The modeled acoustic field at the locale of the VLA as a function of the source range from the VLA at the center frequency of the pass-band, i.e., 200 Hz (see Fig. 17) shows the depth distribution of the TL associated with range-averaged mean square pressure in the last 5 km of the array (upper panel), and the TL from both range and depth-averaged mean-square pressure (lower panel). The modeling results compare quite well with the observed data (see Fig. 16) in many aspects, predicting a gradual decay of the acoustic energy out to approximately 50 km near the shelf break and then followed by an abrupt and severe decay between 50 to 60 km. These similarities are striking considering

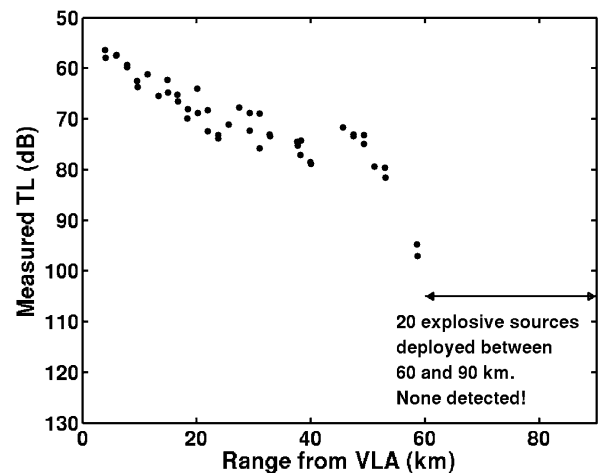


Fig. 16. Measured TL (dB re 1 m) versus the range of explosive source from VLA. The TL shown was derived from the depth-averaged mean-square pressures. Note the rapid and severe drop of signal energy between 54 and 58 km.

that only a rough geoacoustic-parameter model was used. These also suggest that the sediment does not play a primary role in controlling the abrupt degradation, but the Kuroshio front does.

This abrupt signal degradation can be easily explained using normal mode theory. The shallow sound channel on the shelf can only trap a finite number of propagating modes. In fact, the maximum number increases more-or-less linearly from 3 at 100 Hz to 25 at 1 kHz at the VLA site. On the shelf, all the trapped modes span the entire shallow water-column. However, these “shelf” trapped modes begin to occupy a lower portion of the ocean interior near the shelf edge due to the significant increases in the vertical sound-speed gradients seaward, resulting from the presence of the Kuroshio front. The turning depth of a mode approximately defines the vertical extent of the mode stretching from the bottom. Since the initial loudness (i.e., excitation) of a mode is relative to the mode function evaluated at the source depth, the mode is not excited if the source depth is shallower than its turning depth. Also since turning depth decreases as mode number increases, if a higher mode is not excited due to the shallowness of the source, none of the lower modes are excited. Thus, an examination of the turning depths of the shelf-trapped modes is helpful in understanding the excitation or extinction of modal energy.

The turning depths of both the median and highest-order shelf trapped modes as a function of source range from the VLA for various frequencies, 100 Hz to 1 kHz at a 50 Hz increment, are both approximately frequency-independent, i.e., nondispersive (see Fig. 18). For a source located above the turning depth of the highest-order shelf trapped mode, none of those propagating modes on the shelf are excited, causing total signal extinction on the shelf. For a source depth of 50 m, the total extinction is predicted to begin at about 60 km (see Fig. 18). For a source located near the turning depth of the median-order shelf trapped mode, only the upper half of those propagating modes is excited. Recognizing that the energy in the upper half generally attenuates much more rapidly in range than the lower half, sharp decreases in the signal level on the shelf are anticipated when the source depth is close to the turning depths of these median-order shelf

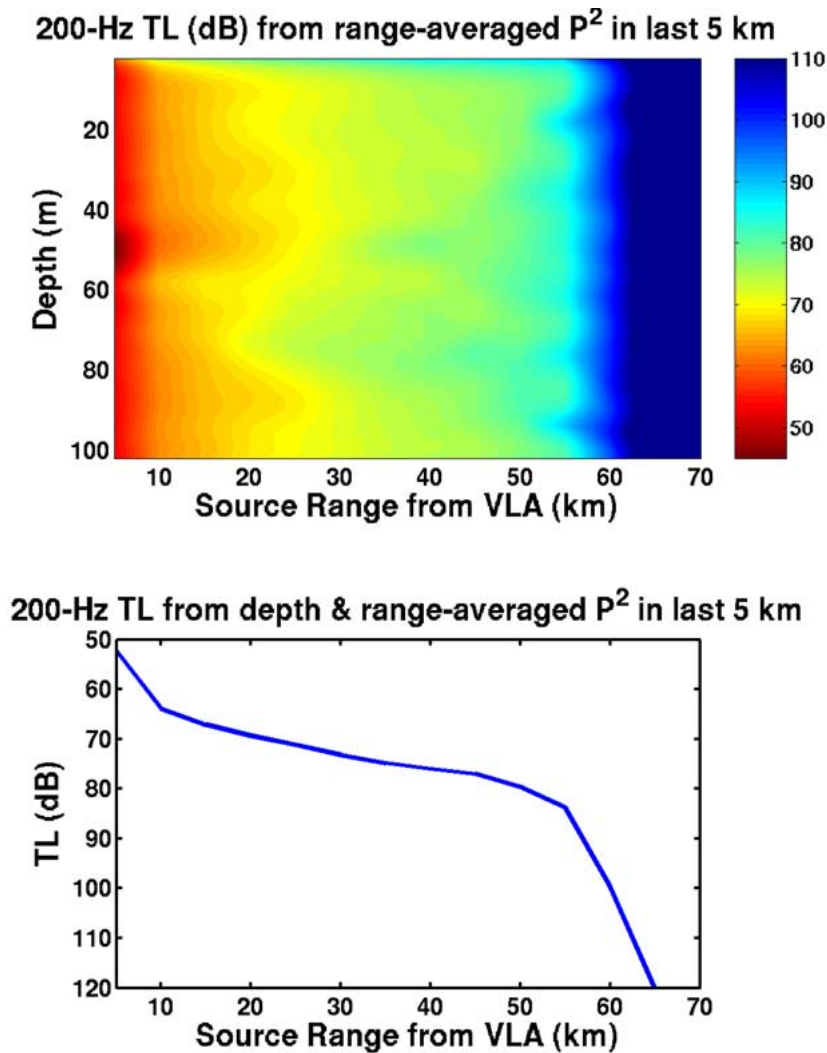


Fig. 17. Modeled 200-Hz TL (dB re 1 m) at the locale of the VLA as a function of source range. The upper panel shows the depth distribution of the TL calculated from range-averaged mean-square pressure in the last 5 km of the array. The lower panel shows the TL from both range and depth-averaged mean-square pressure.

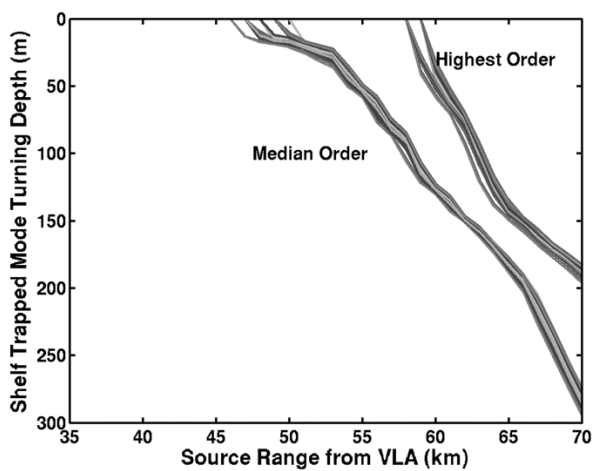


Fig. 18. Turning depths of both the median and highest-order trapped modes on the shelf as a function of source range from the VLA. The curves in each cluster are for various frequencies, 100 Hz to 1 kHz at a 50 Hz increment.

trapped modes. Thus, for a source depth of 50 m, severe signal degradation is predicted to occur around 55 km (see Fig. 18).

What would happen if the profiles were less downward refracting, mimicking a situation when the front has moved sea-

ward? It has been shown that the range at which abrupt signal loss occurs depends primarily on the local upper turning depths of the shelf trapped modes relative to the depth of the source. Weaker vertical gradients would cause the turning depths to rise near the shelfbreak and on the slope. This would essentially result in a translation of the curves in Fig. 18 to the right. Therefore, the range of abrupt loss would increase accordingly as the front translates seaward.

VIII. SUMMARY AND CONCLUSIONS

Data from two field experiments are combined to evaluate the impact of the East China Sea shelf-edge environment on low-frequency acoustic propagation. These are the ASIAEX pilot study during April 2000 and the primary ASIAEX boundary interaction study from May–June 2001, both conducted in the central East China Sea in the region bounded by 28° to 30°N , $126^\circ 30'$ to 128°E . During April 2000, an anchor station and two across-shelf CTD sections were obtained, as well as a short, five-day mooring record and hull-mounted ADCP data. Extensive geology and geophysics observations were collected as well, including mapping the bottom and sub-bottom with water guns, chirp sonars, and sediment cores.

In terms of the 2001 study, this paper focuses only on the broadband acoustic propagation measurements made during June 3–5 and incorporates a subset of the 2001 environmental observations in the form of CTD and XBT data collected during the same period.

A broad range of space and time scales were apparent in the environmental observations. The dominant mesoscale feature during both years was the Kuroshio current that closely follows the continental slope in this region. The inshore (NW) edge of the current was quite pronounced and extended over the edge of the shelf break and up onto the shelf. The edge of the current translated onshore during the first part of the 2000 experiment then moved offshore during the last few days. The current also spawned some small, shallow filaments or “shingles” that extended still farther up onto the continental shelf causing anomalously warm, salty conditions there. The internal tide was also quite prominent in the time series data during both 2000 and 2001, causing 3°C thermal fluctuations semidiurnally at mid-depth. Internal waves were also evident both years, but quite different in their respective structure. During 2000, a packet of nonlinear internal solitons was spawned at the shelf break during a period when the Kuroshio was translating offshore, causing the off-shelf flow to become supercritical. This never happened during 2001 and an energetic field of ordinary oscillatory internal waves was present instead. In terms of the mean fields, the ECS study region over the shelf was warmer and fresher during June 2001 than during April 2000. This was due to increased seasonal warming later in the year during 2001 combined with a more southward extension of the Yangtze River plume.

Two case studies in the acoustic transmission loss (TL) over the continental shelf and slope were performed. First, the anchor station data obtained during 2000 was used to study the acoustic variance induced by a warm filament shed by the Kuroshio Current in the transmission loss (TL) along the seafloor in the NW quadrant of the ECS ASIAEX box. This modeled single-frequency TL structure consisted of significant fine-scale variability in time caused primarily by the changes in the multipath/multimode interference pattern. The interference was quite sensitive to small changes in the phase differences between individual paths/modes induced by the evolution of the warm filament. The resultant standard deviations at various ranges were about 4–5 dB, but could be reduced exponentially by using bandpassed signals in wide enough bands.

Second, the environmental data from both years were combined to obtain a “best picture” of the across-shelf T/S structure during June 2001, which was used to explain the observed phenomenon of abrupt signal extinction as the transmission range lengthened seaward. This abrupt and severe signal degradation was caused by the Kuroshio frontal gradients that produced an increasingly downward-refracting sound-speed field seaward from the shelf break. This abrupt signal dropout was explained using normal mode theory and was predictable and source depth dependent. For a source located above the turning depth of the highest-order shelf trapped mode, none of the propagating modes on the shelf were excited, causing total signal extinction on the shelf.

ACKNOWLEDGMENT

The ASIAEX project was carried out under sustained multi-year funding provided by the Ocean Acoustics Program of the Office of Naval Research, whose support is gratefully acknowledged. The authors thank the officers and crew of the research vessels ROGER REVELLE, MELVILLE, SHI YAN 2, and SHI YAN 3 for their assistance and skill in executing the work at sea. The hard work of the technical support staffs of the Applied Physics Laboratory/University of Washington, the Marine Physical Laboratory/Scripps Institution of Oceanography, the Woods Hole Oceanographic Institution, and the Naval Postgraduate School is much appreciated by all the principal investigators. The authors also wish to thank Phil Abbot who provided helpful advice on how to estimate absolute TL from explosive sources.

REFERENCES

- [1] P. H. Dahl, R. Zhang, J. Miller, L. Bartek, Z. Peng, S. Ramp, J.-X. Zhou, C.-S. Chiu, J. Lynch, J. Simmen, and R. C. Spindel, “Overview of Results from the Asian Seas International Acoustics Experiment in the East China Sea,” *IEEE J. Oceanic Eng.*, vol. 29, pp. 920–928, Oct. 2004.
- [2] J. H. Miller, L. R. Bartek, G. R. Potty, D. Tang, J. Y. Na, and Y. Qi, “Sediment properties in the East China Sea,” *IEEE J. Oceanic Eng.*, vol. 29, pp. 940–951, Oct. 2004.
- [3] L. Rainville and R. Pinkel, “Observations of energetic high-wave number internal waves in the Kuroshio,” *J. Phys. Oceanogr.*, vol. 34, pp. 1495–1505, 2004.
- [4] Z. Peng, J.-X. Zhou, P. H. Dahl, and R. Zhang, “Seabed acoustic parameters from dispersion analysis and transmission loss in the East China Sea,” *IEEE J. Oceanic Eng.*, vol. 29, pp. 1038–1045, Oct. 2004.
- [5] C.-S. Chiu, J. H. Miller, and J. F. Lynch, “Forward coupled-mode propagation modeling for coastal acoustic tomography,” *J. Acoust. Soc. Amer.*, vol. 99, pp. 793–802, 1996.
- [6] B. Qui, T. Toda, and N. Imasato, “On kuroshio front fluctuations in the East China Sea using satellite and in situ observational data,” *J. Geophys. Res.*, vol. 95, pp. 18 191–18 204, 1990.
- [7] Y. Hsueh, J. Wang, and C. S. Chern, “The intrusion of the Kuroshio across the continental shelf northeast of Taiwan,” *J. Geophys. Res.*, vol. 97, pp. 14 323–14 330, 1992.
- [8] Y. Hsueh, C. S. Chern, and J. Wang, “Blocking of the Kuroshio by the continental shelf northeast of Taiwan,” *J. Geophys. Res.*, vol. 98, pp. 12 351–12 359, 1993.
- [9] O. Katoh, K. Morinaga, and N. Nakagawa, “Current distributions in the southern East China Sea in summer,” *J. Geophys. Res.*, vol. 105, pp. 8565–8574, 2000.
- [10] H. Ichikawa and R. C. Beardsley, “Temporal and spatial variability of volume transport of the Kuroshio in the East China Sea,” *Deep-Sea Res.*, vol. 40, pp. 583–605, 1993.
- [11] M. Feng, H. Mitsudera, and Y. Yoshikawa, “Structure and variability of the Kuroshio current in the Tokara Strait,” *J. Phys. Oceanogr.*, vol. 30, pp. 2257–2276, 2000.
- [12] T. Matsuno, T. Hibiya, S. Kanari, and C. Kobayashi, “Small scale internal waves and turbulent fluctuations near the continental shelf break in the East China Sea,” *J. Oceanogr.*, vol. 53, pp. 259–269, 1997.
- [13] G. A. Jacobs, H. B. Hur, and S. K. Reidlinger, “Yellow and East China Seas response to winds and currents,” *J. Geophys. Res.*, vol. 105, pp. 21 947–21 968, 2000.
- [14] C. Chen, R. C. Beardsley, and R. Limeburner, “The structure of the Kuroshio southwest of Kyushu: Velocity, transport, and potential vorticity fields,” *Deep-Sea Res.*, vol. 39, pp. 245–268, 1992.
- [15] C. James, M. Wimbush, and H. Ichikawa, “Kuroshio meanders in the East China Sea,” *J. Phys. Oceanogr.*, vol. 29, pp. 259–272, 1999.
- [16] R. Hickox, I. Belkin, P. Cornillon, and Z. Shan, “Climatology and seasonal variability of ocean fronts in the East China, Yellow, and Bohai Seas from satellite SST data,” *Geophys. Res. Lett.*, 2001.
- [17] S.-H. Lee and R. C. Beardsley, “Influence of stratification on residual tidal currents in the Yellow Sea,” *J. Geophys. Res.*, vol. 104, pp. 15 679–15 701, 1999.

- [18] R. C. Beardsley, R. Limeburner, H. Yu, and G. A. Cannon, "Discharge of the Changjiang (Yangtze River) into the East China Sea," *Cont. Shelf Res.*, vol. 4, pp. 57–76, 1985.
- [19] L. H. Larsen, G. A. Cannon, and B. H. Choi, "East China Sea tide currents," *Cont. Shelf Res.*, vol. 4, pp. 77–103, 1985.
- [20] M.-K. Hsu, A. K. Liu, and C. Liu, "A study of internal waves in the China Seas and Yellow Sea using SAR," *Cont. Shelf Res.*, vol. 20, pp. 389–410, 2000.
- [21] P. Dahl, "ASIAEX East China Sea: Cruise Report of the Activities of the R/V MELVILLE, 29 May to 9 June, 2001," Applied Physics Laboratory, University of Washington, Tech. Memorandum TM 7-01, July, 2001.
- [22] Z. Peng, R. Zhang, and J. Zhou, "ASIAEX, East China Sea. Overview of the Activities and Data Measure of SHIYAN-2 and SHIYAN-3, June 2 to June 7, 2001," National Laboratory of Acoustics, Institute of Acoustics, Chinese Academy of Sciences, Tech. Rep. NL-ME-02-01, 2002.
- [23] J. R. Apel, J. R. Holbrook, A. K. Liu, and J. J. Tsai, "The Sulu Sea internal soliton experiment," *J. Phys. Oceanogr.*, vol. 15, pp. 1625–1651, 1985.
- [24] M.-K. Hsu and A. K. Liu, "Nonlinear internal waves in the South China Sea," *Canadian J. Remote Sensing*, vol. 26, pp. 72–81, 2000.
- [25] A. R. Osborne and T. L. Burch, "Internal solitons in the Andaman Sea," *Science*, vol. 208, pp. 451–460, 1980.
- [26] J. Small, "A nonlinear model of the shoaling and refraction of interfacial solitary waves in the ocean. Part I: Development of the model and investigations of the shoaling effect," *J. Phys. Oceanogr.*, vol. 31, pp. 3163–3183, 2001.
- [27] J. A. Colosi, R. C. Beardsley, J. F. Lynch, G. Gawarkiewicz, C.-S. Chiu, and A. Scotti, "Observations of nonlinear internal waves on the outer New England continental shelf during the summer shelfbreak primer study," *J. Geophys. Res.*, vol. 106, pp. 9587–9601, 2001.
- [28] T. P. Stanton and L. A. Ostrovsky, "Observations of highly nonlinear internal solitons over the continental shelf," *Geophys. Res. Lett.*, vol. 25, pp. 2695–2698, 1998.
- [29] A. K. Liu, J. R. Holbrook, and J. R. Apel, "Nonlinear internal wave evolution in the Sulu Sea," *J. Phys. Oceanogr.*, vol. 15, pp. 1613–1624, 1985.
- [30] S. R. Ramp, T.-Y. Tang, C.-S. Chiu, J. F. Lynch, A. K. Liu, and Y.-J. Yang, "Internal solitons in the northeastern South China Sea Part I: Sources and deep water propagation," *IEEE J. Oceanic Eng.*, vol. 29, pp. 1157–1181, Oct. 2004.
- [31] A. K. Liu, T.-Y. Tang, Y. Zhao, and S. R. Ramp, "A case study of solitary internal wave propagation during ASIAEX-2001," *IEEE J. Oceanic Eng.*, vol. 29, pp. 1144–1156, Oct. 2004.
- [32] J. R. Apel, M. Badiey, C.-S. Chiu, S. Finette, R. Headrick, J. Kemp, J. F. Lynch, A. Newhall, M. H. Orr, B. H. Pasewark, D. Tielbuerger, A. Turgut, K. von der Heydt, and S. Wolf, "An overview of the 1995 SWARM Shallow-water internal wave acoustic scattering experiment," *IEEE J. Oceanic Eng.*, vol. 22, pp. 465–500, 1997.
- [33] A. Scotti and R. C. Beardsley, "Large internal waves in Massachusetts Bay. Part I: Modeling generation, propagation, and shoaling," *J. Geophys. Res.*, submitted for publication.
- [34] C. Chen, R. C. Beardsley, R. Limeburner, and K. Kim, "Comparison of winter and summer hydrographic observations in the Yellow and East China Seas and adjacent Kuroshio during 1986," *Cont. Shelf Res.*, vol. 14, pp. 909–929, 1994.
- [35] I. Dyer, "Statistics of sound propagation in the ocean," *J. Acoust. Soc. Amer.*, vol. 48, pp. 337–345, 1970.
- [36] N. C. Makris, "The effect of saturated transmission scintillation on ocean acoustic intensity measurements," *J. Acoust. Soc. Amer.*, vol. 100, pp. 769–783, 1996.



Steven R. Ramp received the M.S. degree in physical oceanography from the University of Washington, Seattle, in 1976 and the Ph.D. degree in physical oceanography from the University of Rhode Island, Narragansett, in 1986.

Since 1986, he has been with the U.S. Navy as a Professor at the Naval Postgraduate School, Monterey, CA, and a Program Officer at the Office of Naval Research, Arlington, VA. Prior to this, he spent time at the National Marine Fisheries Service, Woods Hole, MA. His research specialty

is ocean observations from both ships and oceanographic moorings, and he has organized major expeditions to the Japan Sea, East China Sea, and South China Sea. He was the International Scientific Coordinator for the Asian Seas International Acoustics Experiment (ASIAEX).



Ching-Sang Chiu received the B.S. degree in electrical engineering from Northeastern University, Boston, MA, in 1979 and the Sc.D. degree in oceanographic engineering from the Massachusetts Institute of Technology, Cambridge/Woods Hole Oceanographic Institution, Woods Hole, MA, joint program in 1985.

He is a Professor of oceanography at the Naval Postgraduate School, Monterey, CA. His research interests include ocean acoustics, acoustical oceanography, and coastal ocean processes and their influence on acoustic prediction. He has authored or coauthored more than 40 refereed publications in those subject areas.

Dr. Chiu is a Fellow of the Acoustical Society of America and Editor-in-Chief of the *Journal of Computational Acoustics*.



Frederick L. Bahr received the M.S. degree in physical oceanography from Oregon State University in 1991.

He was with Oregon State University for two years, where he worked for Dr. Clayton Paulson. He then moved to Bermuda and was with the Bermuda Biological Station for Research for five years as part of the Bermuda Atlantic Time-Series (BATS) project and the Hydrostation S time series. He has been with the Oceanography Department, Naval Postgraduate School, Monterey, CA, for the

past six years.



Yiquan Qi received Doctor of Science degree in physical oceanography from Ocean University of Qingdao, China, in 1998.

Since 1992, he has been a member of the faculty of the Key Laboratory of the Tropical Marine Environmental Dynamics (LED) at the South China Sea Institute of Oceanology, Chinese Academy of Sciences, Beijing, China. He has more than 30 publications in the area of remote sensing and its application in physical oceanography.



Peter H. Dahl received the Ph.D. degree in ocean engineering from the Massachusetts Institute of Technology, Cambridge/Woods Hole Oceanographic Institution, Woods Hole, MA, Joint Program in Oceanography and Oceanographic Engineering in 1989.

He currently is a Principal Engineer at the Applied Physics Laboratory, University of Washington, Seattle, where he has been since 1989, and conducts experimental and theoretical research in underwater acoustics. He also is a Research Associate Professor

in the Mechanical Engineering Department, University of Washington. In 2002, he was a Guest Professor with the Department of Physics, University of Bergen, Norway.

Dr. Dahl served as an Associate Editor for the IEEE JOURNAL OF OCEANIC ENGINEERING from 1997 to 2003 and has served as Guest Editor for this Special Issue on Asian Marginal Seas. He is a Fellow of the Acoustical Society of America (ASA) and currently is Chair of the ASA Technical Committee on Underwater Acoustics. He was the U.S. Chief Scientist for ASIAEX East China Sea.



James H. Miller (S'83–M'87) received the B.S. degree in electrical engineering from Worcester Polytechnic Institute, Worcester MA, in 1979, the M.S. degree in electrical engineering from Stanford University, Stanford, CA, in 1981, and the Ph.D. degree in oceanographic engineering from the Massachusetts Institute of Technology, Cambridge/Woods Hole Oceanographic Institution, Woods Hole, MA, joint program in 1987.

He was a Member of the Faculty, Department of Electrical and Computer Engineering, Naval Postgraduate School (NPS), Monterey, CA, from 1987 to 1995. Since 1995, he has been a Member of the Faculty, Department of Ocean Engineering, University of Rhode Island (URI), Narragansett, where he holds the rank of Professor. He is a Founder of FarSounder, Inc., Providence, RI, a startup company that develops forward-looking sonar for vessels, underwater vehicles, and divers. He has authored more than 100 publications in the areas of acoustical oceanography, signal processing, and marine bioacoustics. He has served as Associate Editor for Underwater Sound for the *Journal of the Acoustical Society of America*, responsible for scattering, inverse methods, and fish acoustics.

Dr. Miller was elected a Fellow of the Acoustical Society of America in 2003 and is a Member of Sigma Xi, Tau Beta Pi, Eta Kappa Nu, the Acoustical Society of America, and the Marine Technology Society. From 2001 to 2003, he was a Member of the National Academy of Sciences Panel on Noise in the Ocean. He serves on the National Marine Fisheries Service Panel on Acoustic Criteria for Marine Mammals. He also serves on the Marine Mammal Commission Subcommittee on the Impacts of Acoustics on Marine Mammals. He received the NPS Menneken Faculty Award for Excellence in Scientific Research and the URI Marshall Award for Faculty Excellence in Engineering in 1993 and 1999, respectively.



James F. Lynch (M'96–SM'03) was born in Jersey City, NJ, on June 3, 1950. He received the B.S. degree in physics from Stevens Institute of Technology, Hoboken, NJ, in 1972 and the Ph.D. degree in physics from the University of Texas, Austin, in 1978.

He was with the Applied Research Laboratories, University of Texas at Austin (ARL/UT) from 1978 to 1981, after which he joined the scientific staff at the Woods Hole Oceanographic Institution (WHOI), Woods Hole, MA. He has been with WHOI since then and currently holds the position of Senior Scientist in

the Applied Ocean Physics and Engineering Department. His research specialty areas are ocean acoustics and acoustical oceanography, but he also greatly enjoys occasional forays into physical oceanography, marine geology, and marine biology.

Dr. Lynch is a Fellow of the Acoustical Society of America and Editor-in-Chief of the *IEEE JOURNAL OF OCEANIC ENGINEERING*.



Renhe Zhang was born in Chongqing, China. He graduated from the Department of Physics, Beijing University, Beijing, China, in 1958.

From 1990 to 2000, he was the Director of the National Laboratory of Acoustics at the Chinese Academy of Sciences (CAS), Beijing, China. He is now an Academician at Institute of Acoustics, CAS.

Prof. Zhang is a Chairman of the Western Pacific Commission for Acoustics and a Member of International Acoustic Commission. He has received Zhu Kezheng, Rao Yutai, Guanghua, and Heliang Heli

awards for contributions to ocean acoustics in China.



Ji-Xun Zhou graduated from the Physics Department, Nanjing University, Nanjing, China, with a five-year degree in 1963 and graduated from the Graduate School of the Chinese Academy of Sciences (CAS), Beijing, China, associated with the Institute of Acoustics (IOA), for a four-year degree in 1967.

He started his research on shallow-water acoustics with the IOA and was promoted to Full Professor. Since April 1989, he was officially appointed as a Visiting Professor and, later, as a Principal Research

Scientist with the Georgia Institute of Technology (Georgia Tech), Atlanta, where he has been advising postdoctoral fellows and Ph.D./M.S. students and visiting scholars. In recent years, his main areas of research have included acoustic interactions with internal waves, sea-bottom geoacoustic inversion, and reverberation and signal spatial coherence in shallow water.

Prof. Zhou was twice awarded the China Natural Science Award (both were 2nd place), as a coauthor, in 1982 and 1989 due to his contributions to shallow-water acoustics.